The Planetary Science Journal, 6:182 (22pp), 2025 August https://doi.org/10.3847/PSJ/adea6a

Plume Activity on Europa: Current Knowledge and Search Strategy for Europa Clipper

Lorenz Roth[1], Erin Leonard[2], Kelly Miller[3], Matt Hedman[4], Lynnae C. Quick[5], Tracy M. Becker[3,6], Shawn Brooks[2], Corey Cochrane[2], Ashley Gerard Davies[2], Carolyn M. Ernst[7], Cyril Grima[8], Candice J. Hansen[9], Carly Howett[9,10], Sean Hsu[11], Xianzhe Jia[12], Adrienn Luspay-Kuti[7], Margaret Kivelson[12,13], Fabian Klenner[14], Alfred McEwen[15], William B. McKinnon[16], Robert T. Pappalardo[2], Frank Postberg[17], Julie Rathbun[18], Kurt D. Retherford[3,6], Kirk Scanlan[19], K. Marshall Seaton[2], John R. Spencer[20], J. Hunter Waite[21], Paul Withers[22,23], Danielle Wyrick[3], and Mikhail Yu. Zolotov[24]
the Europa Clipper Plume Focus Group

[1] KTH Royal Institute of Technology, SE-100 44 Stockholm, Sweden
[2] Jet Propulsion Laboratory, California Institute of Technology, Pasadena, CA 91109, USA
[3] Southwest Research Institute, 6220 Culebra Road, San Antonio, TX 78238, USA
[4] University of Idaho, 875 Perimeter Drive, MS 0903 Moscow, ID 83844-0903, USA
[5] NASA Goddard Space Flight Center, 8800 Greenbelt Road, Greenbelt MD, 20771, USA
[6] University of Texas at San Antonio, 1 UTSA Circle, San Antonio, TX 78249, USA
[7] Johns Hopkins Applied Physics Laboratory, Laurel, MD, USA
[8] University of Texas Institute for Geophysics, University of Texas, Austin, TX, USA
[9] Planetary Science Institute, 1700 E. Fort Lowell, Suite 106, Tucson, AZ 85719, USA
[10] University of Oxford, UK
[11] Laboratory for Atmospheric and Space Physics, University of Colorado, 1234 Innovation Drive, Boulder, CO 80303-7814, USA
[12] Department of Climate and Space Sciences and Engineering, University of Michigan, Ann Arbor, MI 48109, USA
[13] Department of Earth, Planetary, and Space Sciences, University of California Los Angeles, Los Angeles, CA 90095, USA
[14] Department of Earth and Space Sciences, University of Washington, Seattle, WA 98195, USA
[15] University of Arizona, 1541 E. University Blvd.Tucson, AZ 85721-0063, USA
[16] Washington University in St. Louis, 1 Brookings Drive, St. Louis, MO 63130, USA
[17] Freie Universität Berlin, Institut of Geological Sciences, Malteserstrasse 74-100, 12249 Berlin, Germany
[18] Cornell University, Ithaca, NY 14853, USA
[19] DTU Space, Technical University of Denmark, Kongens Lyngby, Denmark
[20] Southwest Research Institute, 301 Walnut Street, Suite 400 Boulder, CO 80302, USA
[21] University of Alabama, Tuscaloosa, AL 35487, USA
[22] Department of Astronomy, Boston University, 725 Commonwealth Avenue, Boston, MA, USA
[23] Center for Space Physics, Boston University, 725 Commonwealth Avenue, Boston, MA, USA
[24] School of Earth and Space Exploration, Arizona State University, Tempe, AZ 85287-1404, USA
Received 2025 March 5; revised 2025 June 24; accepted 2025 June 24; published 2025 August 12

Abstract

The presence of cryovolcanic activity in the form of geyser-like plumes at Jupiter's moon Europa is a much-debated topic. As an active plume could allow direct sampling by a passing spacecraft of a potentially habitable interior environment, the detection and analysis of ongoing plume activity would be of the highest scientific value. In the past decade, several studies have interpreted different remote and in situ observations as providing evidence for large gaseous plumes at different locations on Europa. However, definitive proof is elusive, and visible imaging data taken during spacecraft flybys do not reveal clear indications of ongoing activity. After arrival at Jupiter in 2030, the NASA Europa Clipper spacecraft will systematically search for and constrain plume activity at Europa utilizing a variety of investigations and methods during, before, and after close flybys. Given the lack of a confirmed plume detection to date, the Europa Clipper science team has adopted a global plume search strategy, not focusing on any specific geographical area or any specific type of observation. This global search strategy assigns enhanced value to data obtained early in the mission, which allows time for further observations and characterization of any observed plume at later times. Here we describe the current state of knowledge on plume activity, the Europa Clipper search strategy, and the role of various instruments on the Europa Clipper payload in this search.

Unified Astronomy Thesaurus concepts: Natural satellites (Solar system) (1089); Natural satellite atmospheres (2214); Geological processes (2289); Volcanism (2174); Natural satellite surfaces (2208)

1. Introduction

Europa is the smallest of Jupiter's four Galilean moons, and it has the youngest surface with an estimated average age between 40 and 90 Myr. Ongoing geologic activity at Europa may be expressed in myriad ways, including effusive surface flows, active convection within the ice shell, or diapirism. Such processes could appear as anomalously warm areas ("hot spots") on the surface. Signs of current or recent geological activity can pinpoint locations where the ice shell may be particularly thin or where ice shell inhomogeneities like brine pockets may be present. Exchange between the subsurface and

surface environments is crucial to both habitability itself and the investigation of it (e.g., S. D. Vance et al. 2023). A geyser-like plume represents one of the most dramatic ways that recent or ongoing geologic activity may manifest on Europa. Most broadly, a plume occurs when subsurface material is vented from the surface. Plume activity is of particular interest, as it potentially provides (or greatly enhances) the possibility for Europa Clipper or other passing spacecraft to directly probe material from interior environments that may be habitable during flybys. Characterization of the lofted material in combination with modeling can better constrain crucial parameters like composition, redox state, and pH of the interior plume source (e.g., C. R. Glein et al. 2015). At the same time, the input of exogenic material in regions of (plume) activity may provide a biologically useful chemical energy source to subsurface habitats. Searching for present-day plume activity will be the primary focus in this paper, with acknowledgment of other possible forms of current geologic activity.

We review knowledge around potential plume activity on Europa and describe the science team's plans for the NASA Europa Clipper spacecraft (R. T. Pappalardo et al. 2024). Section 2 gives an overview of processes that could drive plume activity and other geologic activity at Europa. In Section 3, previous relevant studies are reviewed. Section 4 describes the planned Europa Clipper investigations related to plume activity, and Section 5 elaborates on the general plume search strategy for Europa Clipper. In Section 6, we provide a summary.

2. Expectations for Plume Activity and Other Active Resurfacing Processes on Europa

Plume eruptions can potentially arise from a variety of cryovolcanic processes (Figure 1) powered by Europa's internal heat. Possible mechanisms include the following:

(1) Pressure-driven fluid flow combined with exsolution of volatiles causes liquid water in the subsurface to become buoyant relative to the ice shell. This might transport volatile-rich water to Europa's low-pressure surface environment.
(2) Ascending diapirs might coincide with tidally generated cracks in Europa's shell, which then transport volatile-rich water to the surface (J. W. Head et al. 1999; C. B. Phillips et al. 2000; S. A. Fagents 2003).
(3) Tidal stresses acting on near-surface crustal fluid reservoirs might cause fractures in the overlaying ice shell, exposing the liquids to the low-pressure environment (S. A. Fagents et al. 2000; S. A. Fagents 2003).
(4) Excess pressure caused by the gradual freezing of crustal fluid reservoirs might also crack the surface ices, exposing the liquids (e.g., E. Lesage et al. 2022).
(5) Eruptive venting associated with chaos formation, or the migration and subsequent crystallization of brine pockets associated with impacts, might also trigger plume eruptions on Europa (C. C. Walker & B. E. Schmidt 2018; G. Steinbrügge et al. 2020a, 2020b).

While the first four mechanisms could release enough energy to result in sizable eruptions and plumes up to 150 km tall (e.g., A. Vorburger & P. Wurz 2021), the mechanism involving brine pockets forming chaos terrain (5) would produce a plume of the order of only a few kilometers in height (e.g., S. A. Fagents et al. 2000). Based on the average impact frequency and impactor size at Europa, it is unlikely that impact events would trigger sizable plume eruptions (L. Roth et al. 2014a). Nevertheless, each of these eruption mechanisms would also result in endogenic heating of the surface that would result in a thermal anomaly.

It might also be possible that a plume could be generated by radiolytic and thermal processes involving electromagnetic radiation, charged particle radiation, or energetic neutral particles impinging on the moon's surface. The dissociation of clathrate hydrates in the icy crust (S. W. Kieffer et al. 2006) could also trigger eruptions with high amounts of other volatile species in addition to water vapor.

Any of these plume-generating processes could give rise to three observable signatures that could be detected by Europa Clipper during an integrated plume search:

(1) Plume gas or vapor, which refers to individual molecules and atoms launched from beneath the surface. The term "vapor" is used for *gaseous* H_2O in the following.
(2) Plume particles, which are solid pieces of material that could be visible either above the surface or as localized deposits on the surface. These are expected to be mostly dust-sized objects of micrometer size and could have a range of compositions. The term "plume particle" is used synonymously with (ice) grain or dust particles throughout this text.
(3) Surface thermal anomalies.

The strength and duration of detectable signatures of each of these parameters will vary based on a variety of factors, including, but not limited to, plume size, plume composition, and eruption duration.

Gases are likely the driving force for eruptions and are thus expected to be a major component of a plume on Europa, with the largest plume containing the most vapor (see Table 2 of L. C. Quick & M. M. Hedman 2020). Based on analogies with Enceladus and the current understanding of Europa's near-surface geology, water vapor is expected to be the primary gas constituent that drives plumes on Europa. However, other volatile compounds such as carbon dioxide, carbon monoxide, sulfur dioxide, and hydrogen peroxide could also play important roles (S. A. Fagents et al. 2000; J. P. Combe et al. 2019; S. K. Trumbo & M. E. Brown 2023; G. L. Villanueva et al. 2023). While the concentration of gases would be highest close to the eruption source, many of these molecules would travel significant distances and in doing so could significantly influence the structure and composition of Europa's tenuous atmosphere (B. D. Teolis et al. 2017b). Gases may also become ionized and give rise to plasma populations that influence Europa's near-surface ionosphere (X. Jia et al. 2018, 2021) or directly affect the interaction of Europa with the plasma environment (A. Blöcker et al. 2016; H. L. F. Huybrighs et al. 2020).

A general difference between water-rich plumes on Jupiter's icy Galilean satellites and Saturn's moon Enceladus (e.g., M. K. Dougherty et al. 2006; C. J. Hansen et al. 2006, 2011) would likely be the plume height. The Galilean satellites are much more massive than Enceladus, and plume material thus requires higher energy to reach the same heights as and to spread as far as at Enceladus. Adapting the Enceladus plume

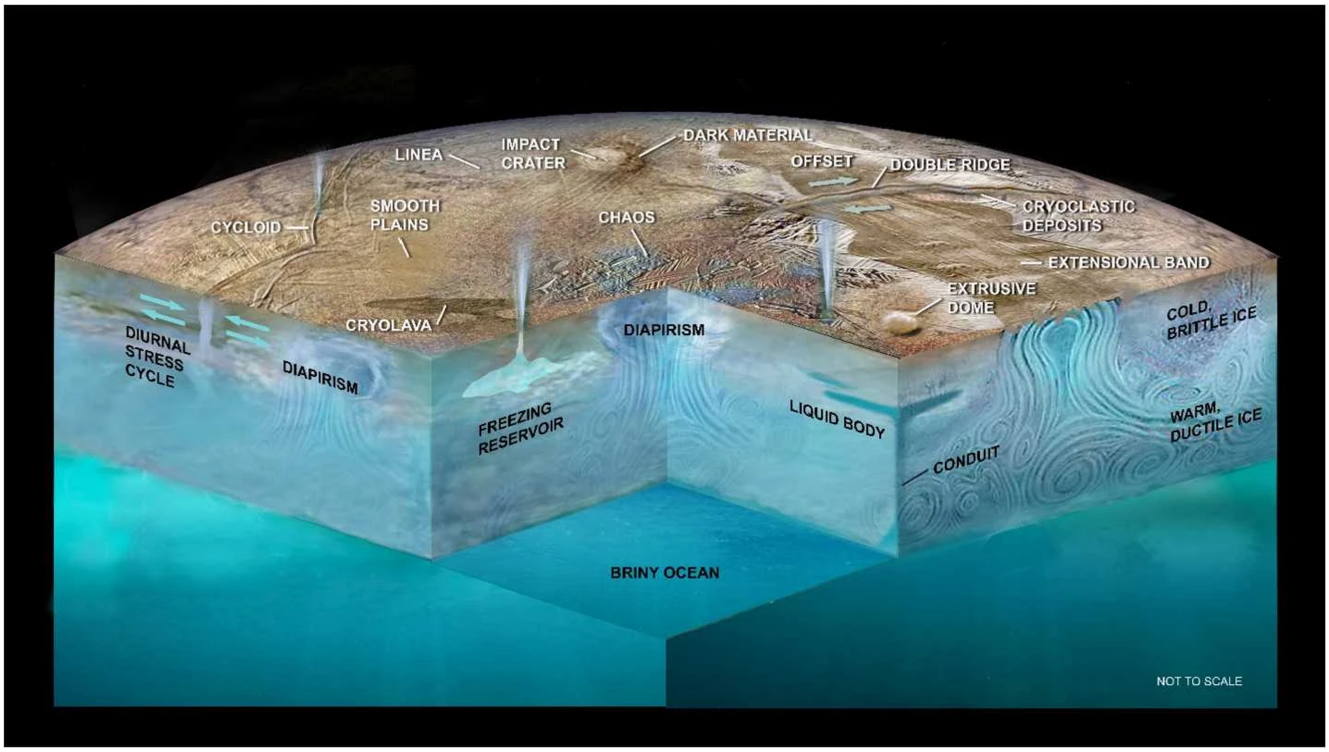

Figure 1. Schematic of a cross section through the icy shell of Europa showing hypothesized processes that might generate a plume, cryovolcanic surface features, and other morphology indicative of current activity. The ice shell is shown as consisting of a cold, brittle shell over a warmer, more deformable ductile layer, above a global briny ocean. The ice shell is subject to stresses that may first form and then possibly open and close cracks and any conduits. The latter could provide indirect pathways for water into the ice shell. These strong tidal stresses contribute to the formation of cycloids, ridges, and extensional bands. The effects of diapirism within the ice shell may penetrate to the surface, leading to extrusion and resurfacing. Diapirism and shell fracturing can lead to the formation of liquid reservoirs within the brittle ice. Stresses in such reservoirs as the water or brine freezes might lead to the opening of conduits to the surface, the generation of a plume, the formation of domes, or the emplacement of "cryolavas" or smooth plains; all these phenomena present the possibility of plume activity to different extents. Figure from I. J. Daubar et al. (2024).

emission mechanism (J. Schmidt et al. 2008) to Europa, whose escape speed is 10 times higher than at Enceladus, a grain dynamics simulation shows that a plume should be more confined in altitude (B. S. Southworth et al. 2015). Eruption processes otherwise being equal, the plume surface deposits on Europa may have a smaller extent, requiring compositional mapping at high spatial resolution to identify them.

While lofted *particles* from actively erupting plumes have not been directly inferred from observations at Europa, particle-rich plumes are found above both Jupiter's moon Io (A. F. Cook et al. 1979; S. A. Collins 1981; J. R. Spencer et al. 2007; P. E. Geissler & M. T. McMillan 2008) and Saturn's moon Enceladus (e.g., C. C. Porco et al. 2006; J. N. Spitale & C. C. Porco 2007; J. R. Spencer et al. 2009), and diffuse patches of fine-grained ice surrounding fissures on Europa's surface could be created by fallen plume material (S. A. Fagents et al. 2000; L. C. Quick et al. 2013). Plume particles might also be lofted by the vapor component. Past work has shown that the plume particle-to-vapor ratio would be highest for plumes that are $\leqslant$25 km tall (L. C. Quick & M. M. Hedman 2020). Putative detections hint at plumes with larger heights of 50–200 km, as discussed in Section 3. Regardless of plume size, larger plume particles (with radii of $\geqslant 1\ \mu$m) are likely to fall back to the surface relatively close to the source and would produce thicker surface deposits than their smaller counterparts. As such, relatively small plumes ($\leqslant$25 km tall, as compared to the larger plumes putatively detected) may also produce surface deposits that are detectable by remote-sensing instruments (L. C. Quick & M. M. Hedman 2020). Remote-sensing observations may therefore identify localized deposits surrounding locations of recent activity, even if the region is not active at the time of observation. Because plumes that produce detectable surface deposits are likely to contain a significant plume particle component, they are also likely to have large-enough optical thicknesses for eruptions to be detected in real time by remote-sensing instruments observing at high phase angles (L. C. Quick et al. 2013) and/or at the terminator (P. E. Geissler & M. T. McMillan 2008). In situ sampling of plume gases or plume particles could provide detailed information about the composition of active plume sources.

Excess subsurface heat accompanying cryovolcanic events or unusual regolith properties caused by the emplacement of plume deposits could cause localized thermal anomalies that could serve as indicators of recent plume eruptions at Europa's surface. For example, at Enceladus, the source regions of the discrete jets composing the plume reveal systematically enhanced heat flow (e.g., C. Howett et al. 2011).

3. Observational Searches for and Possible Detections of an Active or Past Plume

Evidence for plume activity from Europa's near surface or interior has been searched for in spacecraft data and telescopic observations made from Earth and near-Earth space. Here we first describe studies that constrained plume activity from spacecraft imaging and later studies claiming evidence of plume activity from telescope observations. We then

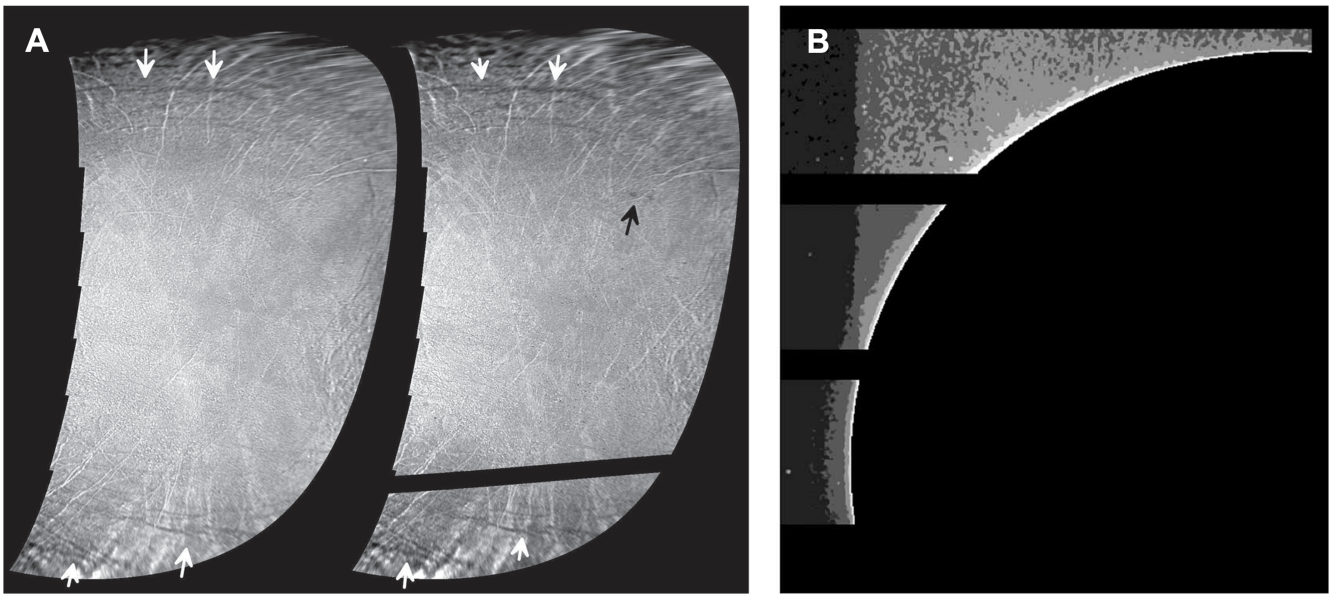

Figure 2. (a) Search for surface changes with Galileo (left) and JunoCam (right) images. White arrows highlight differences in ridges attributed to increased emission angles in the JunoCam images. The black arrow highlights a difference attributed to varied photometric phase functions. (b) Processed JunoCam limb image for high contrast shows no anomalies along the limb (both from C. J. Hansen et al. 2024).

summarize the published results on suggested plume activity from studies using in situ spacecraft data of charged particles and electromagnetic fields at Europa. In the last subsection, we present a brief review on the discovery of the Enceladus plume by the Cassini mission, a potential analog for what might be found on Europa.

3.1. Spacecraft Imaging

Images from the Voyager spacecraft for the first time revealed Europa's surface to be affected by recent geologic activity (B. A. Smith et al. 1979). Hints of activity in Voyager image data, such as detection of bright features, could not be substantiated. Systematic searches for plume activity were not part of the Voyager missions. Using the available (yet limited) imaging data from the Voyager missions and the Galileo mission, C. B. Phillips et al. (2000) carried out a comprehensive study searching for signs of active plumes or surface changes but did not find any concrete evidence. P. M. Schenk (2020) included New Horizons imaging in their search and looked at specific regions from putative detections (see Sections 3.2. and 3.3) but did not find evidence either. Diffuse dark deposits on Europa have been suggested to be past deposits from small plumes (S. A. Fagents et al. 2000; L. C. Quick et al. 2013). Other imaged surface features are consistent with formative mechanisms such as diapirism or tectonic processes (R. T. Pappalardo et al. 1999) but not with large-scale cryovolcanic eruptions (S. A. Fagents 2003).

Analysis of the images taken during the close flyby of the Juno spacecraft did not reveal surface changes (Figure 2(a)) or signs of plumes through light scattered by ejected plume particles near the terminator or limb (Figure 2(b); C. J. Hansen et al. 2024). Such searches have several limitations, e.g., limited spatial coverage, differences in lighting, and/or low spatial resolution of imaging data. However, these searches indicate that plume activity on Europa is neither widespread nor large in scale and may be sporadic.

3.2. Telescope Observations

Hubble Space Telescope (HST) far-ultraviolet spectral observations of Europa taken in 2012 revealed a local emission surplus at atomic hydrogen and atomic oxygen spectral lines (Figure 3, left), consistent with a local source of water vapor at high southern latitude (L. Roth et al. 2014b). The signals extend over more than 1 HST pixel, corresponding to an altitude of >100 km above the surface. Such signals were, however, not detected in two earlier HST spectral images or in follow-up campaigns (L. Roth et al. 2014a, 2022). Using HST with a different observing methodology, W. B. Sparks et al. (2016, 2017) observed Europa in transit of Jupiter and found anomalies along the limb of the moon (Figure 3, right), also extending to at least 50 km above the surface. These anomalies were interpreted by W. B. Sparks et al. (2016, 2017) to be possibly caused by absorption by water vapor or other absorbing substances (other gases or dust particles) erupting from the surface. An independent analysis of the data used in W. B. Sparks et al. (2016, 2017) suggests that the anomalous features could also be created by a small misalignment of Europa's location in the images and/or statistical fluctuations (G. Giono et al. 2020).

Another suggestion of outgassing of H_2O was provided by a detection of infrared emissions from H_2O in 1 out of 17 observations obtained by the Keck telescope (L. Paganini et al. 2020). The amount of H_2O inferred, as well as the transient nature of its detection, led the authors to conclude that outgassing by plumes is the likely source. Sublimation or sputtering as alternative sources for H_2O would produce a more homogeneously distributed source with persistent but low vapor abundance, like that derived later from HST oxygen aurora images (Roth 2021).

Recent studies using data from the Stratospheric Observatory For Infrared Astronomy (SOFIA; W. B. Sparks et al. 2019), the Atacama Large Millimeter/submillimeter Array telescope (M. A. Cordiner et al. 2024), and the Subaru Telescope (J. Kimura et al. 2024) did not confirm the abundance of water vapor or find traces of other gases possibly entrained in plumes.

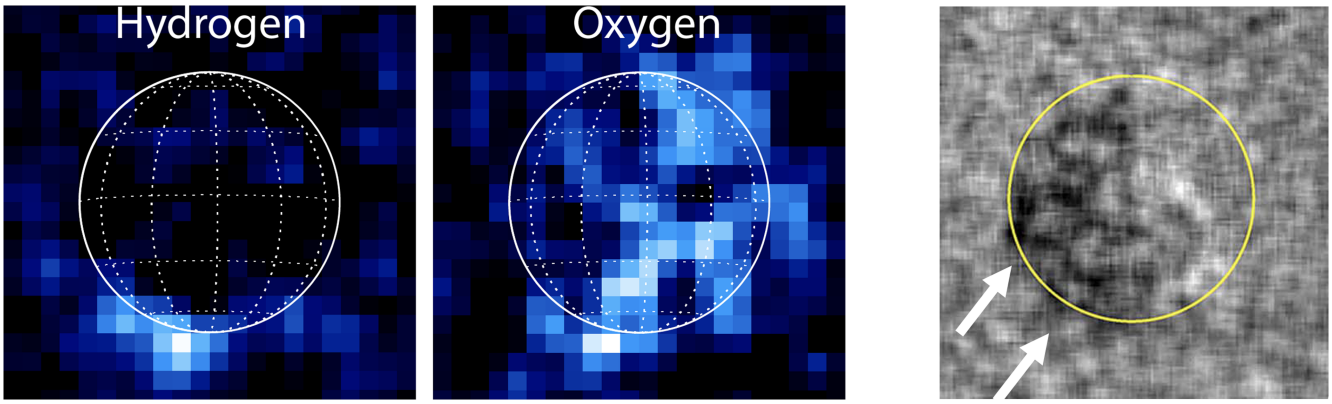

Figure 3. Left: simultaneous spectral HST images of localized emissions from H (at 1215.6 nm) and O (at 130.4 nm) near the south pole interpreted to originate from dissociative excitation of locally sourced H_2O vapor by electrons (adapted from L. Roth et al. 2014b). Right: HST UV filter image of Europa in transit of Jupiter with small dark features outside the yellow circle (white arrows) interpreted to originate from absorption by a substance in erupting plumes (W. B. Sparks et al. 2016). Note that the orbital phase of Europa differs by 90° between these images (the two on the left and the right one) and features appearing on the limb are not mapped to the same locations (see also Figure 4 for the corresponding locations).

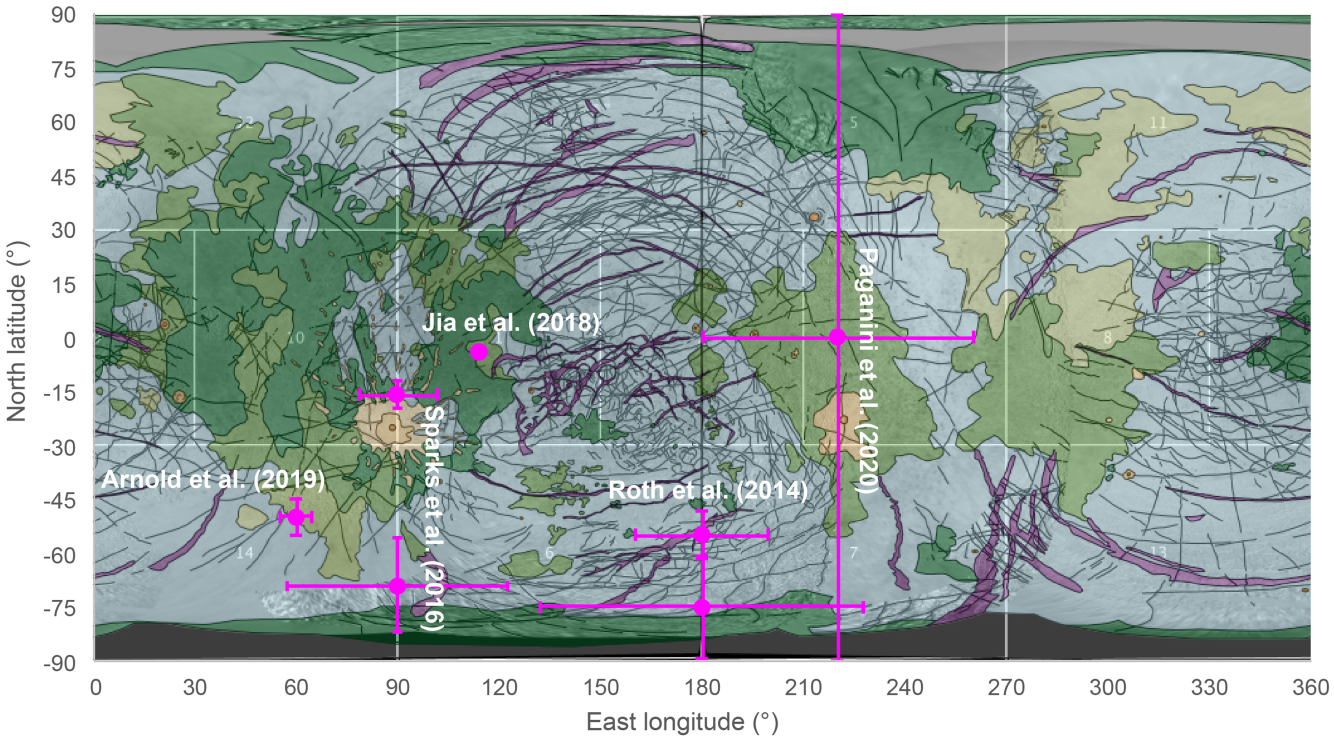

Figure 4. Coordinates of locations of inferred plumes from different studies (pink with error bars indicating the uncertainty) overlaid on a simplified version of the global geological map of Europa (E. J. Leonard et al. 2024). Uncertainties for the coordinates were estimated considering mapping detected features in spatially resolved images to surface coordinates (L. Roth et al. 2014b; W. B. Sparks et al. 2016), the size of the observing slit at the equator (L. Paganini et al. 2020), or the range of parameters tested (H. Arnold et al. 2019). Location and shape of the plume inferred in X. Jia et al. (2018) appear tightly constrained (including a required tilt of the plume axis from the normal), and thus the location has no uncertainty here.

In the first JWST observing program for Europa in 2022, the Near-Infrared Spectrograph (NIRSpec) observed only the leading hemisphere of Europa on 1 day with ∼10 minutes of exposure time (central longitude ∼270°E; see Figure 4), but the data already showed the outstanding capabilities of JWST for probing for plumes and recent activity. The NIRSpec data provide the most stringent constraints so far on the gas, with limits of $<35 \times 10^{30}$ H_2O molecules present on the observed hemisphere. This limit is lower than abundances of published detections by a factor of ∼2–5 (G. L. Villanueva et al. 2023). Furthermore, the spatial (∼10 pixels across the disk) resolution, combined with the spectral information in each pixel, allows detailed studies of local surface composition and possible tracers for activity in the surface such as CO_2 and H_2O_2 (S. K. Trumbo et al. 2019; G. L. Villanueva et al. 2023).

3.3. Spacecraft In Situ Measurements

To date, in situ particle (dust and ice grain) detections in the immediate vicinity of Europa, Ganymede, and Callisto were made with Galileo's Dust Detection System (DDS; E. Grün et al. 1992). H. Krüger et al. (1999, 2000, 2003) analyzed 151 dust particles detected over a total of 16 Galileo flybys (8 of Europa where data were collected). M. Sremčević et al. (2003, 2005)

conclude that these DDS data are consistent with dust particles from impact-generated clouds surrounding these moons. Indications for particles from plume activity were not derived from the DDS data.

Alternatively, analyses of the plasma and electromagnetic field environment have been carried out in the search for signatures from a plume at Europa. Using plasma fluid simulations of Europa's electromagnetic interaction, A. Blöcker et al. (2016) presented a method of searching for magnetic field perturbations arising from a plume as a local inhomogeneity in the global atmosphere but did not find evidence in the Galileo data. Also using fluid simulations, X. Jia et al. (2018) found that a narrow-inclined gas plume produces both a perturbation in the magnetic field and a local plasma density increase. The simulated features are consistent with observed perturbations in the magnetic field and a change in the upper hybrid frequency measured near Europa during the closest Galileo flyby (E12). The simulations are sensitive to the assumed plume density, shape, and extent, which means that the location is also unambiguously constrained (Figure 4). Pointed out a coincidence of the location, where X. Jia et al. (2018) inferred a plume, with a high ionosphere density derived from radio occultation data. H. Arnold et al. (2019), using a hybrid plasma simulation, showed that the magnetic field perturbations measured during another flyby (E26) may have arisen from a plume-like inhomogeneity in the atmosphere. Finally, an absorption feature in measurements of energetic protons by the Galileo spacecraft was proposed to be generated by a plume (H. L. F. Huybrighs et al. 2020) but later shown to be an instrumental artifact (X. Jia et al. 2021).

3.4. Status of Plume Search at Europa

Taken together, the various studies described above show that features detected in different data sets are consistent with plume-like phenomena at Europa, identified through the localized nature of an inhomogeneity (L. Roth et al. 2014b; W. B. Sparks et al. 2016; X. Jia et al. 2018; H. Arnold et al. 2019) and/or through the composition (H_2O) in combination with transient appearance (L. Roth et al. 2014b, L. Paganini et al. 2020). The inferred plumes are all mapped to different locations on the surface, primarily in the southern hemisphere (Figure 4). The signals detected are consistent with large and dense plumes, i.e., reaching high altitudes (>50 km) and/or having high outgassing source rates (e.g., L. Roth et al. 2014b; W. B. Sparks et al. 2016, 2017). All studies that claim plume detections use techniques that are sensitive to and thus measure plume gases (although W. B. Sparks et al. 2016 mention the possibility of dust creating the absorption). All reported remote-sensing detections have low statistical significance (detections on $\sim 3\sigma$–5σ level) and thus are made at the sensitivity limits of the applied techniques. This means that smaller plumes or plumes with lower gas output as assumed in other studies (e.g., S. A. Fagents et al. 2000) would not be detected with these techniques. Dust or ice grain content and altitudes have not been constrained observationally.

Overall, potential plumes were only observed in a small proportion of the total number of observations. Furthermore, follow-up studies on some of the possible plume detections did not substantiate but rather refuted evidence of plume activity. For example, a thermal anomaly on Europa's surface associated with a possible plume detection at these locations was suggested by W. B. Sparks et al. (2017) from HST observations. This area was provisionally associated with a slightly warm area identified in Galileo Photo-Polarimeter Radiometer (PPR) data and proposed as a potential plume source. However, a further analysis of the PPR data (J. A. Rathbun & J. R. Spencer 2020) instead suggested that the location of the anomaly identified by W. B. Sparks et al. (2017) was closer to the ejecta deposit at Pwyll, and the thermal anomaly could instead be explained by passive, reradiated sunlight rather than endogenic activity. Furthermore, one of the recent JunoCam limb images (C. J. Hansen et al. 2024) was obtained near the proposed plume source locations close to the equator from W. B. Sparks et al. (2016) and X. Jia et al. (2018) but did not reveal any indications of plume activity.

Modeling and recent observations have suggested that cryovolcanic venting in the form of geyser-like plumes on Europa may not be dominated by sizable eruptions, that eruptions may be sporadic in nature, and/or that plumes may not be tidally modulated (S. A. Fagents et al. 2000; C. B. Phillips et al. 2000; L. C. Quick et al. 2013; L. Roth et al. 2014a; A. R. Rhoden et al. 2015; L. Paganini et al. 2020). Modeling has also suggested that surface deposits left behind by large plumes may be too diffuse to be detected by spacecraft imagers (L. C. Quick & M. M. Hedman 2020). Given the large uncertainty on the characteristics (vapor/dust content, size, frequency, location, etc.) of a potential Europa plume and the influence of these characteristics on plume detectability by any given measurement technique, utilization of a variety of remote-sensing and in situ instruments is imperative for an unambiguous plume detection at Europa.

3.5. Detection of the Enceladus Plume by Cassini

Detection of the Enceladus plume provides a strong case study for the value of multitechnique plume characterization. The south polar plume at Saturn's moon Enceladus was detected by the Cassini spacecraft during the main mission, and the phenomenon was characterized through a combination of different measurements by various instruments. We briefly review this detection as a potentially interesting reference for Europa and the Europa Clipper mission.

Evidence from Cassini for ongoing plume activity was seen in several data sets obtained during close Enceladus flybys on 2005 February 17 and March 9. As a result of these findings, the altitude of the upcoming 2005 July 14 Enceladus flyby was lowered from the planned 1000 to 169 km, including a UV stellar occultation probing the south polar region. The close July 14 flyby then provided dramatic evidence for current activity: Plume activity and the related phenomena were detected by Cassini's magnetometer (M. K. Dougherty et al. 2006), imaged by the Cassini imaging systems (Imaging Science Subsystem; C. C. Porco et al. 2006) and Ultraviolet Imaging Spectrograph (C. J. Hansen et al. 2006), and sampled by the Ion and Neutral Mass Spectrometer (INMS; J. H. Waite et al. 2006) and Cosmic Dust Analyzer (CDA). The Cassini infrared and thermal imagers (Visual and Infrared Mapping Spectrometer (VIMS) and Composite Infrared Spectrometer (CIRS), respectively) identified and mapped thermal anomalies associated with the plume vents (J. Spencer et al. 2006; C. Howett et al. 2011). Infrared examination of the plume revealed the dominant composition (water ice) and small plume particle sizes. Distant high phase angle (>140°) images

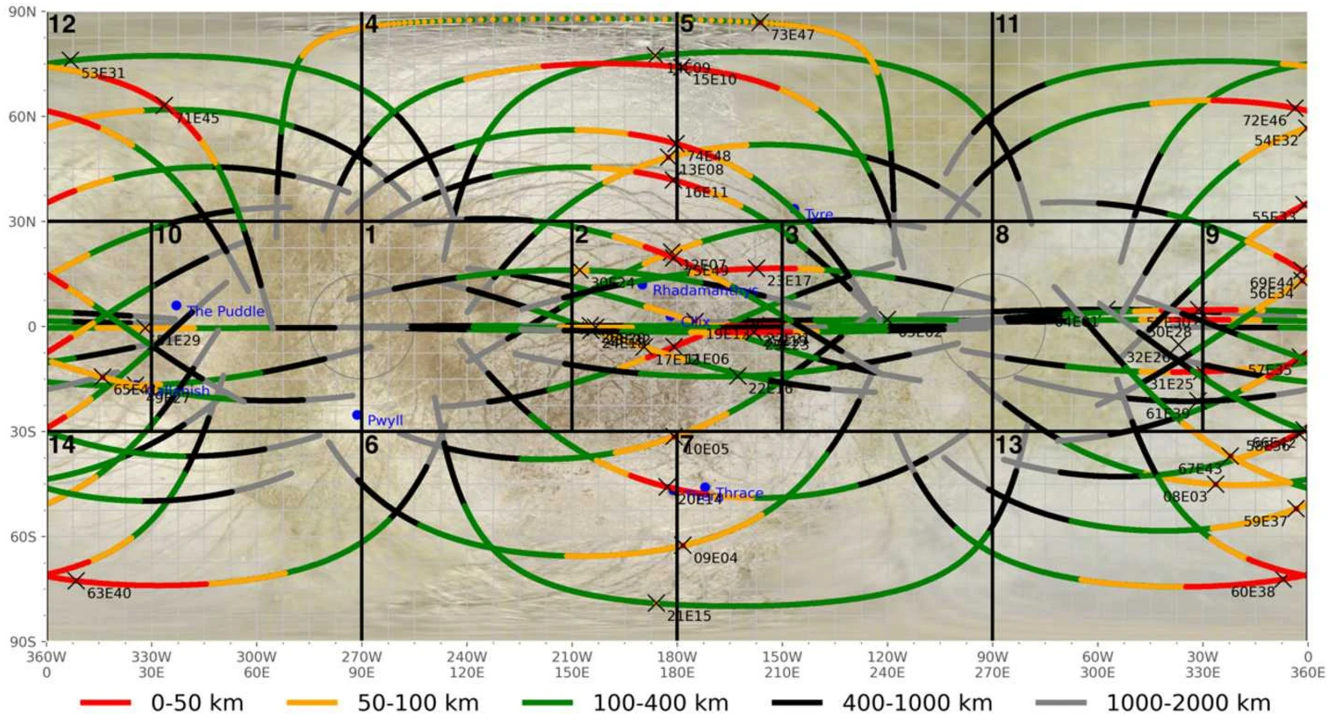

Figure 5. Planned trajectory (21F31_v6) for the Europa Clipper Tour Phase. Each line is the ground track of the spacecraft colored by altitude (up to 2000 km) and labeled by Jovian orbit number and Europa flyby number (e.g., 72E46 is the 72nd Jupiter orbit and the 46th Europa flyby). Crosses show the subspacecraft location for each flyby at closest approach. For more information (such as panels and numbers) on this figure, see details in R. T. Pappalardo et al. (2024).

taken in 2005 November showed the dust plume in detail (C. C. Porco et al. 2006).

As a result of the detection of plume activity, Enceladus became a high-priority target for the first (2008–2010) Cassini extended mission (the Cassini Equinox Mission). The tour for this extended mission was chosen in 2007 February and included seven close Enceladus flybys in addition to the four in the nominal mission. The second extended mission (the Cassini Solstice Mission, 2010–2017) added another 12 close flybys. Flexibility in the plan during the prime Cassini mission and the ability to design an extended mission based on prime mission discoveries resulted in a revolution in our understanding of Enceladus. In particular, the Cassini measurements of plume material led to the conclusion that Enceladus likely contains the necessary ingredients for a habitable environment (e.g., M. L. Cable et al. 2021). Since Cassini's initial set of detections, the Enceladus plume and the water torus formed from the plume gas have been measured from space-based telescopes (P. Hartogh et al. 2011; G. L. Villanueva et al. 2023). Such observations provide means to continuously study Enceladus's activity and possibly guide attempts to search for plume activity at Europa.

4. Europa Clipper Plume-related Investigations

Launched on 2024 October 14, NASA's Europa Clipper will enter Jupiter orbit in 2030 April. It will investigate Europa by flying past the moon 49 times in the prime mission, which lasts until 2034. Figure 5 shows the ground tracks of the flybys, with typical closest-approach distances around 25–100 km. In addition to the general objectives to investigate Europa's interior (ice shell and ocean), composition (T. M. Becker et al. 2024), and geology (I. J. Daubar et al. 2024), Europa Clipper will also search for and characterize current activity, including possible plumes, using its suite of remote-sensing and in situ instruments (R. T. Pappalardo et al. 2024). These science objectives and the tailored investigations using nine scientific instruments and a gravity and radio science investigation enable the Europa Clipper mission to conduct its overarching cross-disciplinary goal to assess Europa's habitability. Table 1 provides a simplified overview of the Europa Clipper instruments and their plume-related measurements. A comprehensive characterization of plume (in)activity at Europa will be achieved through the combination of the different investigations. In the following sections, we explain the contributions of each instrument to the search for and characterization of plume activity and other related forms of current activity.

4.1. EIS

The Europa Imaging System (EIS) is a visible-light imaging system composed of two cameras: the wide-angle camera and the narrow-angle camera (NAC; E. P. Turtle et al. 2024). EIS's primary role in Europa Clipper's integrated plume search strategy is to search for the particle component of potential plumes, both in actively erupting plumes and in the form of surface deposits emplaced by recent plume eruptions. If plume particles are identified, EIS will identify local plume eruption sites on Europa and constrain the properties and eruption frequencies of any plumes observed.

Due to the broad range of possible plume geometries on Europa, and in an effort to maximize the chances of detection, EIS will utilize several methods and a variety of viewing geometries to search for plumes. These methods include (i) imaging along Europa's terminator; (ii) imaging of Europa's bright limb, especially at high phase angles; and (iii) imaging during solar eclipses. Plumes on Europa may be markedly

Table 1
Europa Investigations and Their Plume-related Measurements

(Primary) Investigation Type	Europa Clipper Instrument	Section in This Paper	Primary Constrained Characteristic	Primary Measurement (Technique)	Secondary Measurements
Remote sensing of plume ejecta and surface properties	EIS	4.1	Plume particles	Scattered light from particles	Surface changes and surface deposits, vapor/gas emissions
	Europa-UVS	4.2	Plume gas	Gas emissions and absorptions	Composition and plume-induced variability in environment
	MISE	4.3	Plume surface deposits	Surface reflectance	Plume particle scattering, surface thermal anomaly
	E-THEMIS	4.4	Plume source region	Surface thermal emissions	Surface property changes (albedo and thermal inertia) derived from thermal measurements
In situ probing of plume ejecta	MASPEX	4.5	Plume gas	Gas composition and density including minor compounds	Gas evolved from hypervelocity ice grain impacts inside the instrument
	SUDA	4.6.	Plume particles	Grain composition including salts	Plume deposit or ejected grains
Probing for plumes via effects on the plasma environment	ECM	4.7	Plume gas via ionized particles ("plume ions and electrons")	Local *B*-field perturbations	Ion cyclotron waves from plume pickup ions
	PIMS	4.8		Local plasma enhancement	Detection of water-group ions in environment
	REASON	4.9		Local electron enhancement through relative delays between radar bands	Surface deposit density, roughness, and possibly thickness via the strength of backscattered surface echoes
	G/RS	4.10		Local electron enhancement in radio occultation profiles	

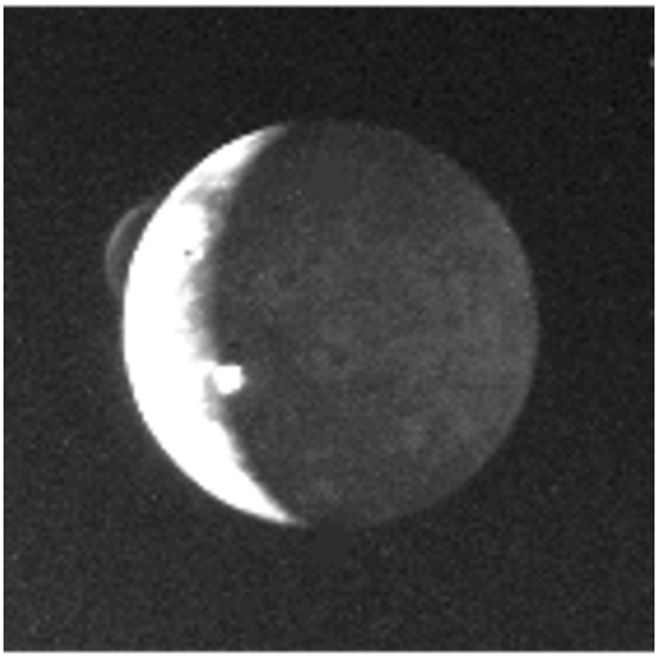

Figure 6. Voyager 1 image of plumes on Io's limb (left) and terminator from a distance of 4.5×10^6 km. Similarly, EIS will be able to detect plumes erupting on Europa's limb and terminator.

different from Enceladus's plumes in terms of the amount of material erupted and eruption frequency (C. J. Hansen et al. 2019). As such, necessary plume detection methods may differ. In order to search for active plumes on Europa, EIS will undertake terminator and limb imaging at 60°–170° phase angles, and up to 180° phase angle during solar eclipses when the spacecraft is in Europa's shadow. If plumes contain a significant fraction of icy particles, they will manifest as bright areas above the limb and/or terminator. Since plume particle size distribution is likely to be dominated by very small particles, the highest phase angles are most promising; however, lower phase angles will also be targeted. Although a bright plume beyond the terminator would be smaller than a plume seen along the limb, a terminator detection would allow for a more accurate determination of the plume source and would allow for identification of smaller plumes, on the order of tens of kilometers tall (Figure 6). Notwithstanding, both limb and terminator detections would facilitate the determination of minimum plume heights.

The EIS NAC will acquire limb and terminator images at 10 km pixel scale or better, which is sufficient to image both smaller plumes that may extend to ~25 km above the surface (S. A. Fagents et al. 2000; L. C. Quick et al. 2013) and large plumes that may be over 100 km high. In the mission tour phase before Europa flybys begin, this search may be extended to lower-resolution images because of the value of early plume detections in planning for future observations.

The EIS team defined measurement requirements to optimize the plume search data set. First, the signal-to-noise ratio (SNR) should exceed 10:1 in the clear (panchromatic) bandpass for an I/F greater than 0.01 (comparable to the brightness of jets on Enceladus). The image scale must be 10 km pixel^{-1} or better (although lower-resolution images will be acquired). Terminator images nominally require phase angles from 60° to 120°, while limb images require phase angles of at least 130°–170° (but images outside these ranges will be acquired). The separation between sampled Europa orbital true anomalies shall be less than every 30° across the full range of orbital true anomalies, because the plumes may vary in intensity throughout Europa's orbital cycle, as at Enceladus (M. M. Hedman et al. 2013). Finally, the separation between sampled longitudes within 60° of the equator shall be less than every 10° across the full range of longitudes, to ensure a thorough global search. These observations will be acquired multiple times throughout the mission to cover the possible duty cycle for transient plume activity proposed in W. B. Sparks et al. (2017). The potential value of the low-resolution images is validated by JunoCam's images of the Tonatiuh plume on Io at a distance of ~300,000 km with a resolution of ~200 km pixel^{-1} (M. A. Ravine et al. 2025).

In addition to direct detections of plumes, change detection with EIS's color filters will also enable a search for fresh plume deposits on Europa's surface. In the absence of direct imaging of active plumes, the identification of plume deposits could provide evidence of recent and/or ongoing plume activity on Europa. Indeed, deposits from plumes that are <30 km tall and that erupt several times per day could grow to be 1–10 m thick over a relatively short timescale (~tens of years), especially in cases where deposits are fluffy (i.e., porosities on the order of 90%; L. C. Quick & M. M. Hedman 2020). Such deposits will be detectable by EIS in clear-filter images. EIS is also capable of detecting much thinner plume deposits, which will be identifiable by their brightness, color, or photometric (see below) contrast with the surrounding surface. Deposits emplaced by much larger plumes could also accumulate enough mass to be detected by EIS, if they are composed of large (e.g., 2–3 μm radius) particles and/or resist compaction (L. C. Quick & M. M. Hedman 2020).

Comparisons between Clipper, Juno, Voyager, and Galileo visible image data will make it possible to identify surface changes that have occurred over a 30 yr period. In order to ensure that accurate comparisons can be made between imagery of the surface acquired by Europa Clipper and the limited number of high-resolution images acquired by Galileo, EIS will make a special effort to reimage areas of Europa's surface that were first imaged by Galileo, ideally with similar illumination and phase angles. Comparisons of EIS imaging at very high resolution (i.e., $\leqslant$10 m pixel^{-1}) over the duration of the mission, even if separated by only a few years, could reveal small-scale changes.

Regions of unusual photometric brightness or behavior will be identified from overlapping images and targeted to search for recent deposition indicative of plume eruptions. Sites of recent activity could exhibit color and albedo anomalies, which would be best observed at less than 60° phase angles, and/or brightness changes due to textural anomalies, which would be observed at high phase angles (i.e., phase angles greater than or equal to 120°). Increased reflectance at high phase angles may indicate areas of recent activity. Low phase angle (<0.1°) observations will be used to look for photometric effects that may indicate fresh plume deposits (R. M. Nelson et al. 2002).

4.2. Europa-UVS

The Europa Ultraviolet Spectrograph (Europa-UVS) observes ultraviolet photons in the 55–206 nm wavelength range at moderate spectral and spatial resolution (K. D. Retherford et al. 2024).

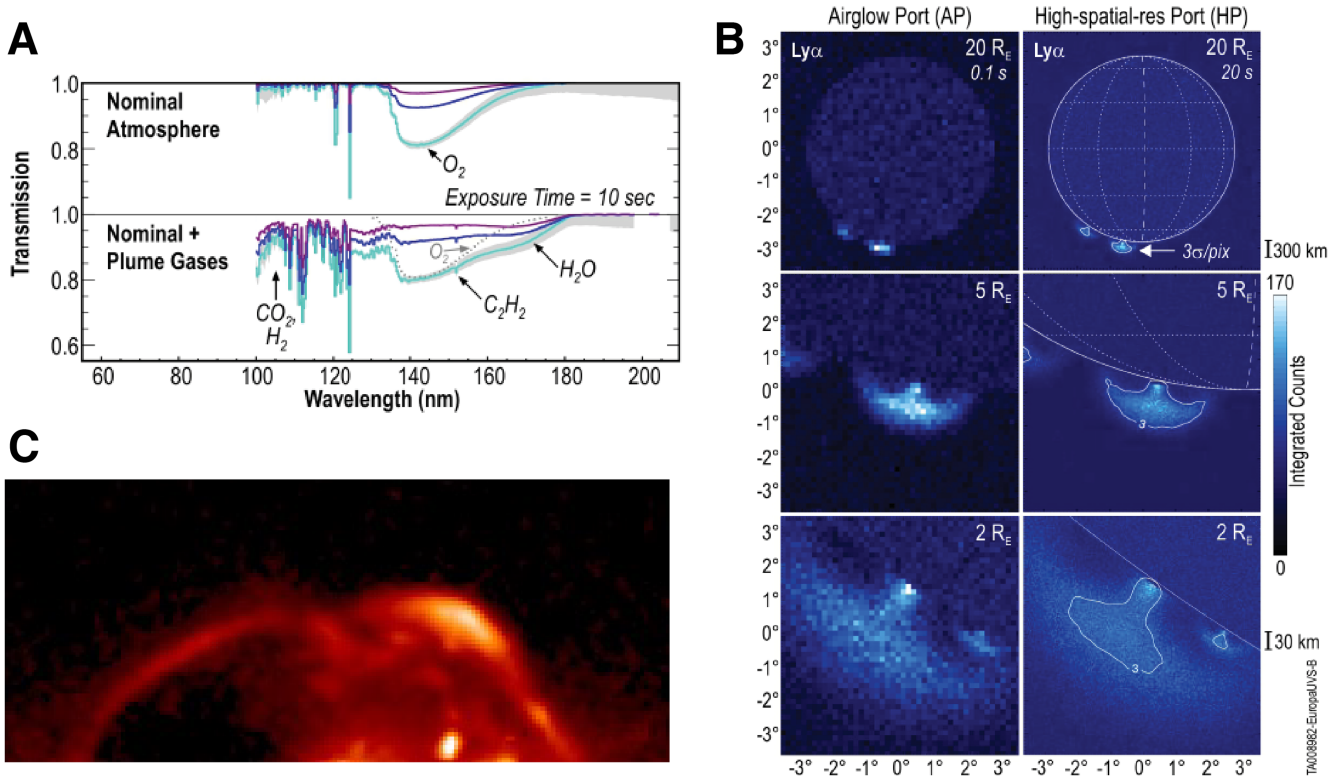

Figure 7. (a) Modeled identification of plume gas and atmospheric gas in absorption during Europa-UVS occultation. (b) Europa-UVS mapping of H Lyα plume auroral emissions as modeled after L. Roth et al. (2014b) using the push broom observing mode with airglow port and high spatial resolution port. (c) New Horizons image of optical auroral emission from Tvashtar plume near Io's north pole (J. R. Spencer et al. 2007).

Europa-UVS is sensitive primarily to detecting water vapor and its dissociation products. Scattering of light by particles is only detectable for Europa-UVS in absorption for very large concentrations. Hence, detecting gaseous plume constituents is the primary means for Europa-UVS to identify the presence of a plume. Europa-UVS will be capable of searching for and characterizing the vapor composition of any plumes that extend 30 km or more above the surface of Europa. Signatures of plume gases are measurable by Europa-UVS in emission and absorption; both signals allow identification of the gas composition through the spectral characteristics.

Europa-UVS's push broom observing method measures surface, aurora, and airglow features during closest-approach periods, which could be used to build a spatial map of a potentially active plume (Figure 7(b)). These features are also imaged from a distance by pointed stares and scanning of Europa's disk, providing observations with the potential to reveal emissions from the water dissociation products within plumes either silhouetted against space (Figure 7(b)), as shown by L. Roth et al. (2014b) with data from HST's Space Telescope Imaging Spectrograph (STIS), or with Europa's disk as the background, as New Horizons eclipse imaging demonstrates (Figure 7(c)). Auroral emissions from large plumes were used to probe the gas composition of Io's plumes (Figure 7(c); L. Roth et al. 2011). The Europa-UVS disk scans will be performed at least six times per flyby on ~70% of Europa encounters, with a goal of obtaining at least six such observations on every flyby in addition to two joint scans with Clipper's other remote-sensing instruments.

Another Europa-UVS plume search measurement will be taken when Europa transits Jupiter's disk. These observations are a powerful means of detecting telltale absorptions by water vapor and potentially other vapor constituents against the backdrop of the planet all along the limb of Europa, as shown for the Enceladus plume against Saturn (C. J. Hansen et al. 2019). Far-UV observations of Europa in transit of Jupiter were used by W. B. Sparks et al. (2016, 2017) and for investigating the atmosphere and searching for plumes with HST (Section 3.2).

In addition, Europa-UVS will acquire atmospheric measurements during at least 100 stellar occultations (M. A. Velez et al. 2024), and the coverage of those occultation observations will be distributed globally around Europa. Should such an occultation intersect an active plume, the observation would provide valuable information about plume composition, density, and structure. This technique would also detect an overall change in the density, extent, or composition of the atmosphere caused by a recent, but no longer active, plume. If present at sufficient levels, constituents such as H_2O, CO_2, O_2, CH_4, NH_3, H_2, and CO_2 will be detected (K. D. Retherford et al. 2024).

Observations of the Sun enabled by Europa-UVS's solar port will obtain additional information on any putative plumes should the mission/plume geometry prove favorable for solar occultations. Because of the Sun's relative brightness compared with stars, solar occultations will enable the detection of trace constituents entrained in the plumes, especially those at wavelengths shortward of 91.2 nm that cannot be observed during stellar occultations owing to absorption by the interstellar medium. Candidate species include but are not limited to those for stellar occultations plus H_2CO, and possibly N_2, C_2H_2, SO_2, and O_3 if densities are higher than expected by analogy with the Enceladus plume.

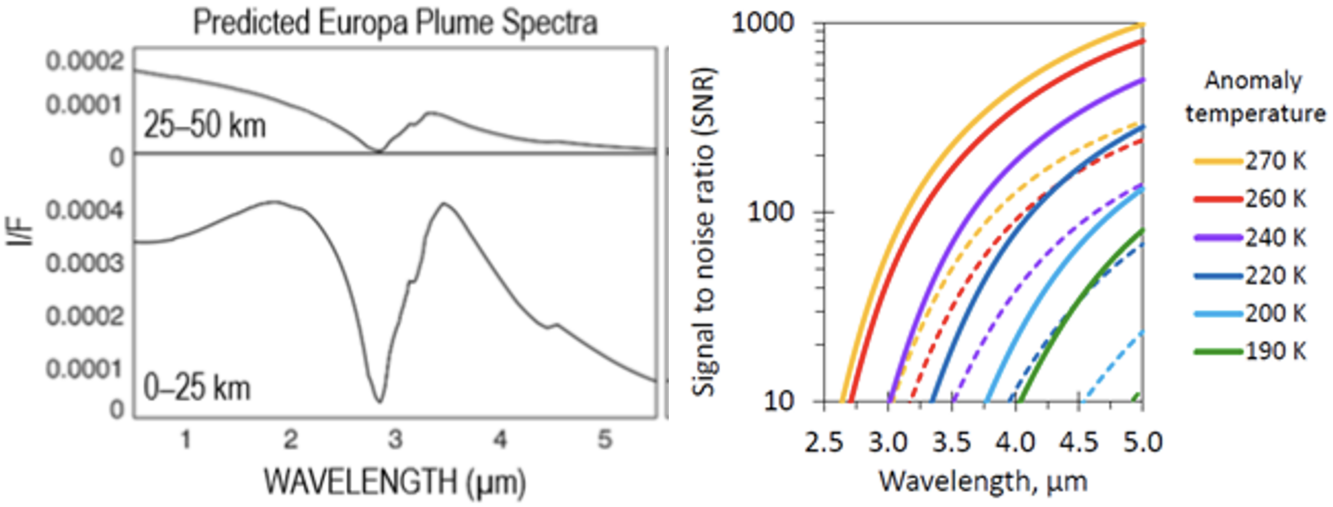

Figure 8. Left: two theoretical MISE spectra of a plume on Europa, computed assuming that the plume particles are composed of pure water ice and that the particles' size and launch velocity distributions are similar to those of the Enceladus plume (D. Blaney et al. 2024). The spectrum of the plume's upper reaches is bluer than that of the base because larger particles are launched at lower speeds (J. Schmidt et al. 2008; F. Postberg et al. 2011). Right: detection of thermal anomalies by MISE (D. Blaney et al. 2024). The solid lines represent a pixel-filling thermal anomaly. The dashed lines represent a 10% pixel fill fraction. The acceptable SNR is 10. Coadding of bands further increases instrument sensitivity.

Additional evidence for plumes may be found in changes to the density or morphology of the neutral clouds surrounding Europa (e.g., L. Roth et al. 2023); Europa-UVS will characterize these clouds twice during each flyby. Finally, surface far-UV reflectance maps may provide a means to identify localized fresh deposits from plume activity.

4.3. MISE

The Mapping Imaging Spectrometer for Europa (MISE) is a high spectral resolution imaging spectrometer covering 0.8–5 μm that is designed to characterize the composition of Europa's surface materials and detect thermal anomalies associated with active resurfacing of Europa (D. Blaney et al. 2024). MISE can use a variety of spectral and photometric indicators to identify (i) recent deposits of plume material on Europa's surface, (ii) lofted grains launched by an active plume, and (iii) thermal anomalies that may be associated with plume sources.

Fresh surface deposits created by recently active plumes can potentially be identified as localized regions that disrupt or overlay global geologic or exogenous effects. In particular, even relatively thin plume deposits (significantly less than 1 mm) could produce detectable spectral signatures if the composition and grain size of the plume particles are sufficiently different from Europa's underlying surface materials. In particular, the small grains in a plume deposit will likely alter the typical scattering length in the regolith, which will in turn affect spectral parameters like ice band depth. Observations by MISE can therefore be used to detect ongoing resurfacing, pinpointing locations for additional study of newly erupted material.

MISE should be able to observe small particles of solid matter lofted above the surface in a plume. If particles in any plume at Europa are as small as those in the Enceladus plumes, they are likely detectable by MISE through remote sensing of forward-scattered light in high phase angle ($>160^\circ$) observations. These high phase angles are also optimal for plume detection because they cause the limb and terminator to be close to each other, potentially allowing the lit plume material to be seen above a dark limb, minimizing stray-light contamination from the surface. In these viewing geometries, absorption bands are suppressed, but MISE should still be able to discern the strong 3 μm water-ice band and thus determine the grain size and composition of the particles in Europa's plumes (Figure 8, left). Spatially resolved, high phase angle spectra should also reveal the spatial distribution of particles with different sizes, which will provide information about the launch velocities of the plume particles (e.g., Hedman et al. 2009). (It is less clear whether MISE will have sufficient spatial resolution and SNR to isolate plume signals near the terminator at lower phase angles.)

If any plume vent sites on Europa are similar to plume sources on Enceladus, thermal anomalies at the vents (J. D. Goguen et al. 2013; J. Spencer et al. 2018) emit sufficient energy in the MISE wavelength range to be detectable. As described elsewhere (D. Blaney et al. 2024), MISE is sensitive to surface thermal anomalies associated with active resurfacing that might generate plumes. MISE would detect such thermal emission between 3 and 5 μm (S. A. Fagents 2003) if the thermal anomaly filled a significant portion of the instrument field of view at a sufficiently high temperature. Detection of thermal features at multiple wavelengths could constrain the temperature and area distribution of the thermal anomaly within the range of detection, all of which would be diagnostic of how the material was physically erupted. Whether MISE detects a thermal anomaly depends on the integrated spectral radiance from the temperature and area distribution within a pixel. For example, MISE could detect the thermal signature with an SNR of 10 for an area at 190 K, if it filled 10% of the MISE field of view (Figure 7(b)). At close approach to Europa (e.g., 50 km), this would be an area of only 16 m^2. MISE could also detect small thermal anomalies with sufficiently high temperature (D. Blaney et al. 2024). MISE and Europa Thermal Emission Imaging System (E-THEMIS) data are complementary in determining the temperature–area distribution of any thermal anomaly detected on Europa's surface. For example, VIMS on Cassini covered an infrared wavelength range similar to MISE.

VIMS detected thermal anomalies on Enceladus associated with plume vents, yielding a temperature of 197 ± 20 K and implied fissure width of 9 m, inferred from thermal emission between 3 and 5 μm (J. D. Goguen et al. 2013).

4.4. E-THEMIS

E-THEMIS is a three-band, thermal infrared imager spanning 7–70 μm (P. R. Christensen et al. 2024). E-THEMIS will support the search for plumes on Europa through three avenues of investigation: (i) by directly detecting the surface heat signature of active plumes, (ii) by detecting and characterizing thermal anomalies of Europa's surface that may be indicative of recent resurfacing and venting, and (iii) by enabling regolith properties such as grain size and thermal inertia to be constrained.

Any active or recent resurfacing activity on Europa will deposit relatively warm material (up to 273 K) that will be at higher temperatures than the nonactive Europa background (peaking at about 130 K), leading to surface thermal anomalies. E-THEMIS is designed to detect thermal emission from such warm areas and down to background minimum nighttime temperatures (around 90 K) with an absolute accuracy of 1–2.2 K (band 1 [7–14 μm] = 2.0 K; band 2 [14–28 μm] = 2.2 K; band 3 [28–70 μm] = 1 K). E-THEMIS will perform the same function at Europa that CIRS on Cassini performed at Enceladus, including the detection of such thermal anomalies. The source of venting on Enceladus has been localized to four ridge-bound fractures dubbed "tiger stripes," which were found to have elevated temperatures (J. Spencer et al. 2006; J. N. Spitale & C. C. Porco 2007; O. Abramov & J. R. Spencer 2009). Heat flow of 4–19 GW (J. Spencer et al. 2006; C. Howett et al. 2011; J. Spencer et al. 2018) was measured from these fractures, emanating mostly at wavelengths beyond 15 μm. Example emitting fracture widths and peak fracture temperatures in regions sampled at high resolution are 9 m at 197 ± 20 K, as inferred from 3–5 μm emission (J. D. Goguen et al. 2013), and 214 m at 167 K (J. Spencer et al. 2018). Similar thermal anomalies on Europa would be detectable by E-THEMIS.

Other surface thermal anomalies may be directly associated with geologic features that give rise to plumes. Europa has a younger average surface age than Enceladus, suggestive of recent widespread resurfacing. However, the formation mechanisms of many surface features are still uncertain (e.g., I. J. Daubar et al. 2024). For example, Europa's ubiquitous double ridges (L. M. Prockter & G. W. Patterson 2009) are potentially analogous to the warm double ridges that are the active vent sources on Enceladus. If these ridges or other regions of Europa are indeed plume sources, then it is plausible that they are currently active and likely warm enough for E-THEMIS to detect. Notwithstanding, the presence of thermal anomalies does not necessarily imply plume activity on Europa (S. K. Trumbo et al. 2018; J. A. Rathbun & J. R. Spencer 2020), and large, vapor-dominated plumes may not produce detectable plume deposits (L. C. Quick & M. M. Hedman 2020).

If an active plume on Europa has a measurable signal at thermal infrared wavelengths, then E-THEMIS could directly detect it. Limb scans acquired as part of the planned global scan will be used to search for off-limb thermal anomalies. However, Cassini's CIRS was unable to detect Enceladus's plumes directly, so it is likely that E-THEMIS will also not be able to detect such a plume at Europa.

Cryoclastic deposits from plume activity may consist of fine particles with potentially low thermal inertia similar to lunar pyroclastic deposits (P. O. Hayne et al. 2017; K. A. Bennett et al. 2018). Recent deposition of fine grains might produce faint thermal anomalies detectable by E-THEMIS. Surface deposition of plume gases could potentially increase thermal inertia by sintering grains together; part of the S/SO_2-rich Pele plume deposit on Io exhibits higher than background temperatures at night (J. Rathbun et al. 2004), possibly due to a high thermal inertia, sintering, or the ongoing emplacement of new material. However, such anomalies need to be distinguished from areas with anomalous thermal inertia values not resulting from plumes or other volcanic activity, such as the high thermal inertia "Pac-Man" anomalies on Mimas, Tethys, and Dione (C. J. A. Howett et al. 2011, 2012, 2014), which are likely due to regolith sintering by electron impact.

In order to derive a surface's thermal inertia and albedo, the daytime and nighttime surface temperatures need to be constrained. The E-THEMIS operational requirements therefore include that 50% of the area covered by the global daytime data set should also be covered by the global nighttime data set and that high spatial resolution observations are made during the day and at night at 15 distinct sites that are well distributed across Europa's surface. Global nighttime coverage by E-THEMIS is required at spatial resolutions close to (or preferably better than) the size of the active region. Figure 9 shows the E-THEMIS global coverage by local time (with night being before 90° and after 270°) for a possible Europa Clipper tour. As shown, E-THEMIS will obtain nighttime coverage at all longitudes. Spatial resolution varies with location (not shown).

4.5. MASPEX

The MAss Spectrometer for Planetary EXploration (MASPEX) is a high mass resolution multibounce time-of-flight mass spectrometer that measures neutral species in Europa's environment with sensitivity for abundances down to sub-parts-per-million (J. H. Waite et al. 2024). MASPEX will make spatially resolved measurements of Europa's exosphere during each flyby, completing a full measurement cycle every 5 s during close approaches. The resulting spatial resolution is directly proportional to the spacecraft's altitude. The minimum planned closest approach of ~25 km provides the greatest spatial resolution for MASPEX measurements. Exosphere volatiles will also be cryotrapped throughout the flybys, and this accumulated sample will be measured subsequent to each flyby at apoapsis. This will enable longer integration times in regions with lower radiation for the measurement of trace compounds. In addition to measurements of the exosphere, ice grains that impact the ceramic strike plate mounted in the instrument antechamber provide another source of neutral gas that will be measured. When an ice grain impact is detected, the MASPEX flight software automatically triggers collection of a set of spectra that are optimized for ice grain compositions before resuming collection of spectra optimized for the exosphere gas.

While MASPEX utilizes an in situ measurement technique, the instrument has the potential to detect a plume without

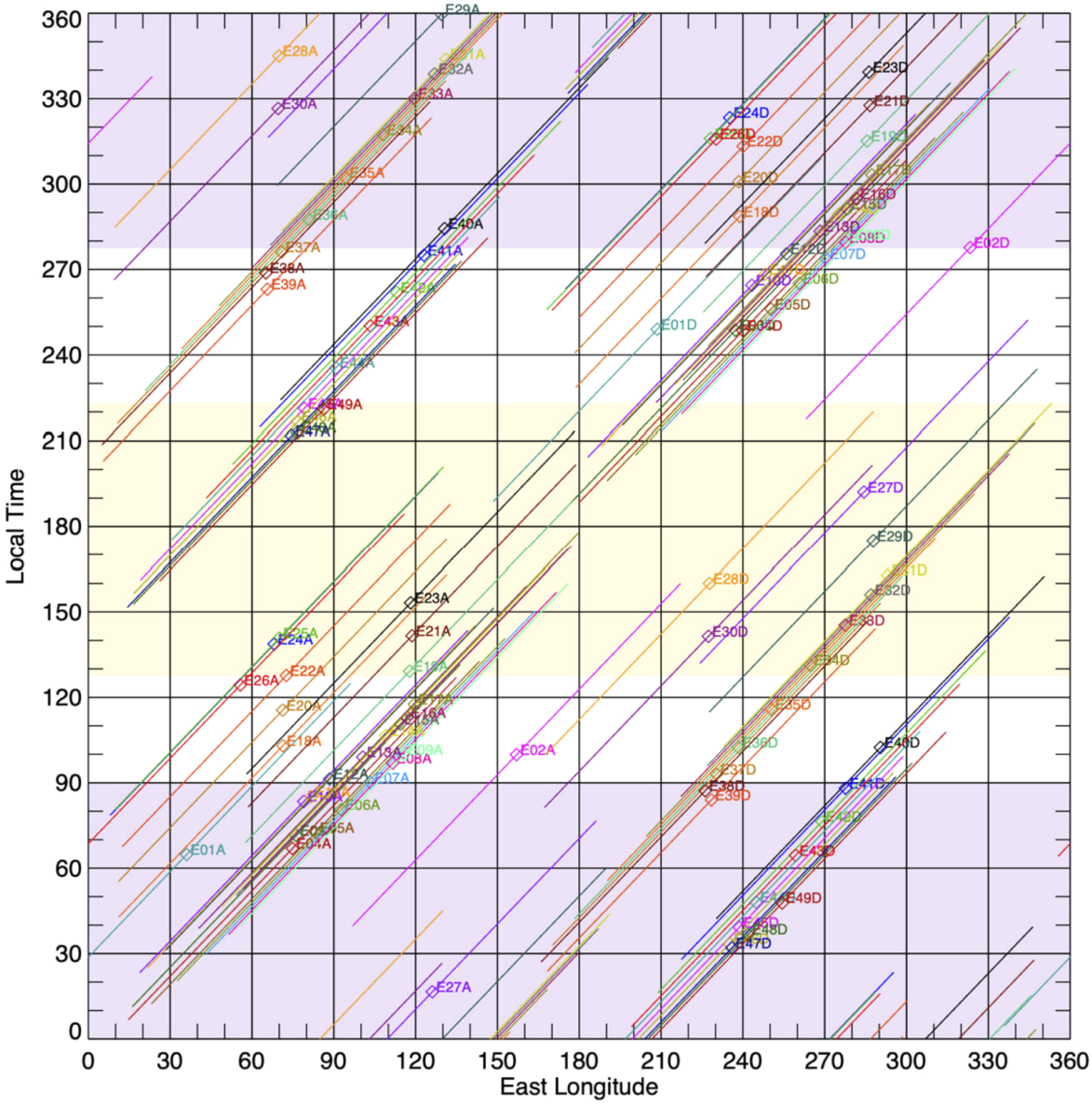

Figure 9. Global coverage of Europa in longitude and local time for a possible tour for Europa Clipper (figure from P. R. Christensen et al. 2024). Local time is measured in degrees of rotation, starting at midnight. Global data are assumed to be obtained during joint scans obtained at roughly 30,000 km range on approach and departure for each flyby. Each diamond represents the subspacecraft point during the approach (suffix "A") or departure (suffix "D") leg of the named orbit, and the diagonal line shows longitude and local time away from the subspacecraft point, out to 60° emission angle. Arbitrary colors are used to distinguish different orbits. Orange and purple background indicates the desired "day" and "night" local times for thermal inertia determination, respectively, as specified in the E-THEMIS requirements.

flying directly through it because of the expected long-range effects of a plume on the exosphere structure and composition. Modeling of the evolution of Europa's exosphere composition with a Monte Carlo simulation of sputtering and thermal desorption of surface molecules in the presence or absence of a plume suggests that a plume not only enhances the local exosphere density but also may alter the exosphere composition even at large distances from the plume source (B. D. Teolis et al. 2017a). For this simulation, the assumed composition of the plume was derived from the observed Enceladus plume composition (J. H. Waite et al. 2009), while the sputtered surface composition was based on existing constraints for Europa's surface. Plume-derived exosphere compositions in B. D. Teolis et al. (2017b) were distinct from both modeled sputtering of water ice at the surface (T. Cassidy et al. 2013) and sputtering of terrain with nonice constituents (T. A. Cassidy et al. 2009; W. M. Grundy et al. 2007). The latter was assumed to include a mixture of sulfate hydrates (R. E. Johnson et al. 2009; J. B. Dalton et al. 2012; M. E. Brown & K. P. Hand 2013), plus organic material modeled after Enceladus. Differences in the modeled exosphere composition and spatial structure result not only from the assumed compositions but also from surface processes such as sublimation, differential transport, surface adherence, and radiolysis of the assumed compositions (B. D. Teolis et al. 2017a). While the potential effect of a plume on Europa's neutral torus (A. Lagg et al. 2003; B. H. Mauk et al. 2003; H. T. Smith et al. 2019) is poorly constrained, existing models suggest that the water mass ejected by a plume is significant compared to a neutral water torus generated solely by H_2O

Table 2
MASPEX Example Decision Table for the Investigation Objective Addressing the Search for and Characterization of a Plume

Species Ratio/O_2	H_2O	CH_4	C_2H_4	C_2H_6	HCN
Ratio decision value	>15	$>3.5 \times 10^{-3}$	$>10^{-3}$	$>10^{-1}$	$>10^{-4}$
1. Plume contribution to exosphere	true	true	true	true	true
2. Radiolytic new terrain	false	true	true	false	true
3. Radiolytic old terrain	false	false	false	false	false

Note. Specific criteria and ratios will be updated as exploration of Europa by the full instrument payload provides additional insight. The "ratio decision value" characterizes the ratio of each compound column to O_2. Detection of a plume requires all five ratio criteria to be met.

molecules from the sputtered or sublimated atmosphere (Q. Nénon & F. Leblanc 2024). Planned MASPEX measurements of the neutral torus and its composition may therefore also help to identify plume activity.

At Enceladus, the closest analogous measurements of the plume were made by the Cassini INMS. Although INMS had lower mass resolution, mass range, and measurement cadence compared to MASPEX, its results provide valuable insights into what MASPEX could reveal about a potential Europa plume. INMS data provided critical insight into the plume composition (J. H. Waite et al. 2006; J. H. Waite et al. 2009; F. Postberg et al. 2018a), including minor compounds such as CO_2, CH_4, and N_2 that constrain the redox state and pH of the source aqueous environment (C. R. Glein et al. 2008; C. R. Glein et al. 2015; C. R. Glein & J. H. Waite 2020). Critically, INMS data identified the presence of H_2 gas in disequilibrium with CO_2 and CH_4, signaling an available chemical source of energy for biotic methanogenesis (J. H. Waite et al. 2017). High-velocity ice grain impacts with the instrument antechamber produced volatiles, and INMS measurements complemented CDA data on more refractory organic compounds contained within ice grains in the E ring (F. Postberg et al. 2018b; N. Khawaja et al. 2019). Data from the INMS within the Enceladus plume revealed critical insights into the plume source's organic chemistry (J. H. Waite et al. 2009; A. Bouquet et al. 2019). Additionally, INMS measurements of neutral gas densities provided constraints on the structure of the gas and dust components of the plume (B. Teolis et al. 2010; M. E. Perry et al. 2015) and enabled estimates of the plume's production rate (H. Smith et al. 2010; Y. Dong et al. 2011; B. D. Teolis et al. 2017a; S. K. Yeoh et al. 2017). At Europa, anomalous $CO_2/CH_4/H_2O$ ratios in the local exosphere could indicate a plume and its source, whether crustal or oceanic (T. M. Becker et al. 2024). Radiolysis of ice forms H_2, and characterizing Europa's habitability will require greater dependence on the use of organic compound ratios to infer characteristics of the internal ocean, including pH, oxidation state, potential hydrothermal temperature, and metabolic potential.

The recommended characteristics for recognition of an active plume, sputtering of freshly deposited material, and old surfaces are summarized in Table 2. Compounds are ratioed to O_2, a major exosphere component expected to dominate in the absence of a plume except in cases like a dense sublimation component near the subsolar point. These detection criteria are, therefore, independent of the exospheric density. Localized density enhancements that are not attributed to solar irradiation, radiolytic processes, or other periodic phenomena may serve as an in situ detection criterion. If each of the ratio decision values shown is exceeded (all "True"), this would suggest that a plume is currently active somewhere on Europa's surface. If all ratios are below the decision value (all "False"), then the exospheric chemistry is consistent with an exosphere composition radiolytically generated from old terrain. The second case ("radiolytic new terrain") suggests that while there may not be an active plume during a given flyby, the exosphere composition reflects sputtering from freshly deposited material. The specific compound ratios listed in Table 2 assume that the plume is Enceladus-like in composition, dominated by water and including reduced organic compounds present at the level of $\sim 10^{-3}$. Compounds detected by MASPEX that contrast with the overall surface composition can be classified as shown in Table 2 to help reach a conclusion as to the origin of this variation in composition. Less massive compounds are especially useful because of their greater scale height, enhancing detectability at higher altitudes. Similarly, compounds more resistant to photolysis and radiolysis would persist as observable plume signatures for a longer period after venting. Conversely, detection of compounds with poor survivability under surface conditions could signal recent activity.

4.6. SUDA

The SUrface Dust Analyzer (SUDA) is an impact ionization mass spectrometer that provides elemental and molecular composition of ice and dust particles around Europa (S. Kempf et al. 2024). Outgassing events from icy moons that create a gas plume likely also entrain microscopic ice grains in the gas, lofting grains to altitudes accessible during close flybys of Clipper (e.g., B. S. Southworth et al. 2015). SUDA will perform in situ particle characterization along the spacecraft trajectory, including composition and size distributions. The number of electric charges and grain speeds with respect to the spacecraft will also be measured by SUDA's entrance grid system.

SUDA's effort regarding plume science during the prime mission is an integral part of its primary task: compositional mapping of Europa's surface. Along the spacecraft trajectory ground track during each flyby, SUDA will measure ejecta particles lofted into the exosphere by micrometeoroid impacts (A. V. Krivov et al. 2003). Each ejecta grain serves as a sample from its source on the surface, the area of which is constrained through the grain's velocity vector, allowing the origin of the grain on Europa's surface to be determined with a spatial resolution dependent on the spacecraft flyby altitude. The SUDA measurements of grain composition along a flyby path therefore enable the mapping of surface composition, with the potential to infer compositional ground truth for features observed on Europa (F. Postberg et al. 2011; W. Goode et al. 2021, 2023). Utilizing flybys with ground tracks covering overlapping locations, SUDA will monitor surface composition changes over the Clipper prime mission. If an ejecta grain population with a composition resembling plume deposits (e.g., S. Kempf et al. 2010) is identified during a later flyby, a plume eruption near the ground track that has occurred between these two flybys can be identified and further investigated.

The surface composition mapping and monitoring effort is particularly important over geologically young terrains (e.g., P. Matteoni et al. 2023a, 2023b) with crossover opportunities such that both anions and cations can be investigated. Figure 10 shows ground track coverage over these regions from crossover flybys. These include Thera and Thrace (during E14 and E51 flybys), Rathcroghan Chaos (E06, E12, E50), and Goirias Chaos (E13, E17, E24, E49). We note that E50 and E51 are not part of the prime mission (R. T. Pappalardo et al. 2024).

If measurements can indeed be obtained while flying through an active plume, grain size and speed information will help to examine both the plume eruption mechanism and the material deposition pattern on the surface. Upon hitting the instrument's target plate, ions produced by the dust grain impact will be analyzed by time-of-flight mass spectrometry. The compositional and dynamical information obtained by SUDA by flying through an active plume will provide direct constraints about both the plume's physical status and its chemical makeup and will complement observations from other instruments in studying the current level of geoactivity on Europa and resurfacing processes. Mass spectra of plume grains will provide constraints on the physical status of the plume source (solid/liquid/clathrate) and critical geochemical connections to Europa's subsurface waters (pH, salinity) and the moon's potential habitability. If a plume is driven by a liquid source, the potential of such measurements to investigate Europa's habitability has been demonstrated with Cassini's CDA at Enceladus. Although the capabilities (e.g., mass resolution, sensitivity) of CDA were inferior to SUDA by far, the instrument provided numerous critical insights regarding the composition, temperature, and pH of Enceladus's subsurface waters, as well as its organic inventory (N. Khawaja et al. 2019). Analog experiments suggest that instruments like SUDA are even capable of identifying biosignatures, if present in ice grains that are emitted from a plume on Enceladus or Europa (e.g., F. Klenner et al. 2020; F. Klenner et al. 2024).

For SUDA, observing an active plume will likely require low-altitude flybys, preferably at or below 100 km altitude (Figure 11). Note that even during such a low-altitude flyby a plume's signature will overlap with the background ejecta cloud population and may require a comprehensive compositional and dynamical analysis for a clear separation of these two sources. This can be achieved by, for example, comparing grain flux and composition profiles, as well as grain mass/speed distributions with the ejecta cloud model throughout the flyby.

4.7. ECM

The Europa Clipper Magnetometer (ECM) consists of three, three-axis fluxgate sensors that measure the vector magnetic field over a wide dynamic range of ±4000 nT per axis (M. G. Kivelson et al. 2023). Together with the Plasma Instrument for Magnetic Sounding (PIMS, Section 4.8), ECM will be capable of identifying and characterizing plumes encountered on passes with closest approach lower than ∼400 km if the spacecraft passes close to or through a plume. Charge exchange interactions of plume neutrals with flowing plasma and impacts of energetic electrons and ions trapped in Jupiter's magnetospheric magnetic field ionize some fraction of the plume's neutral population. It is the ionized portion of a plume that can carry current and thereby interact with the magnetized plasma that continually flows onto the trailing hemisphere of Europa. The interaction changes both plasma and magnetic field on a spatial scale characteristic of the width of the plume, i.e., smaller than the radius of the moon.

A plume is expected to cause localized rotation and compression of the magnetic field and a short-lived increase of plasma density. Such signatures were found in Galileo spacecraft data acquired near the closest approach on the E12 flyby of Europa, an exceptionally low altitude pass. The magnetometer recorded a significant increase of field magnitude accompanied by rapid field rotations lasting about 3 minutes. At the peak of the perturbation, a short-lived electron density enhancement was identified (X. Jia et al. 2018). A magnetohydrodynamic simulation (X. Jia et al. 2018) that incorporated a plume reproduced the dominant field and plasma perturbations with reasonably good fidelity. If an active plume is present during one of the multiple low-altitude passes of the Europa Clipper spacecraft, its signature should be evident in ECM and PIMS measurements.

Newly ionized neutrals from a plume can produce unstable plasma distributions that generate ion cyclotron waves. Near Europa, Jupiter's field is roughly 500 nT and ion cyclotron frequencies fall in the single-digit to sub-Hz range (depending on the ion mass and charge). Such waves can be identified in magnetometer data (M. Volwerk et al. 2001). Wave polarization depends on the sign of the ion charge. Positively charged ions (expected to dominate) will generate left-hand-polarized cyclotron waves. The 16-sample-per-second rate of ECM is ideal for measuring the properties of newly ionized particles. The measured frequency can confirm PIMS measurements of particle mass per charge and provide constraints on the composition of the plume.

4.8. PIMS

PIMS measures the plasma contribution to the magnetic field perturbations sensed by ECM (Section 4.7.) with four Faraday Cup plasma spectrometers (J. Westlake et al. 2023). PIMS is capable of identifying a plume by detecting in situ ionization products as Europa Clipper flies through the plume. The first set of ions PIMS is expected to detect are the water-group ions, which would show up as current peaks at specific energies.

Besides this direct detection of plume signals, PIMS could detect the ionospheric and magnetospheric impact of a plume even after the plume itself is no longer active. This capability is highly valuable in case the detection of an active plume is missed and would enable focused attention on a specific area with recent plume activity that otherwise would not be detectable. This could be accomplished by detecting water-group parent ions, which are not expected to originate from normal Europa activity or normal atmospheric loss to the environment and would most likely be remnants of plume activity. In addition to compositional inference of the impact of a plume on the environment, PIMS can detect changes in the ionosphere and adjacent magnetospheric plasma environment that indicate recent enhanced ionization (above the standard level). The capability will improve as Europa Clipper conducts more flybys and develops an improved characterization of the average/expected ionospheric and near-magnetosphere environment.

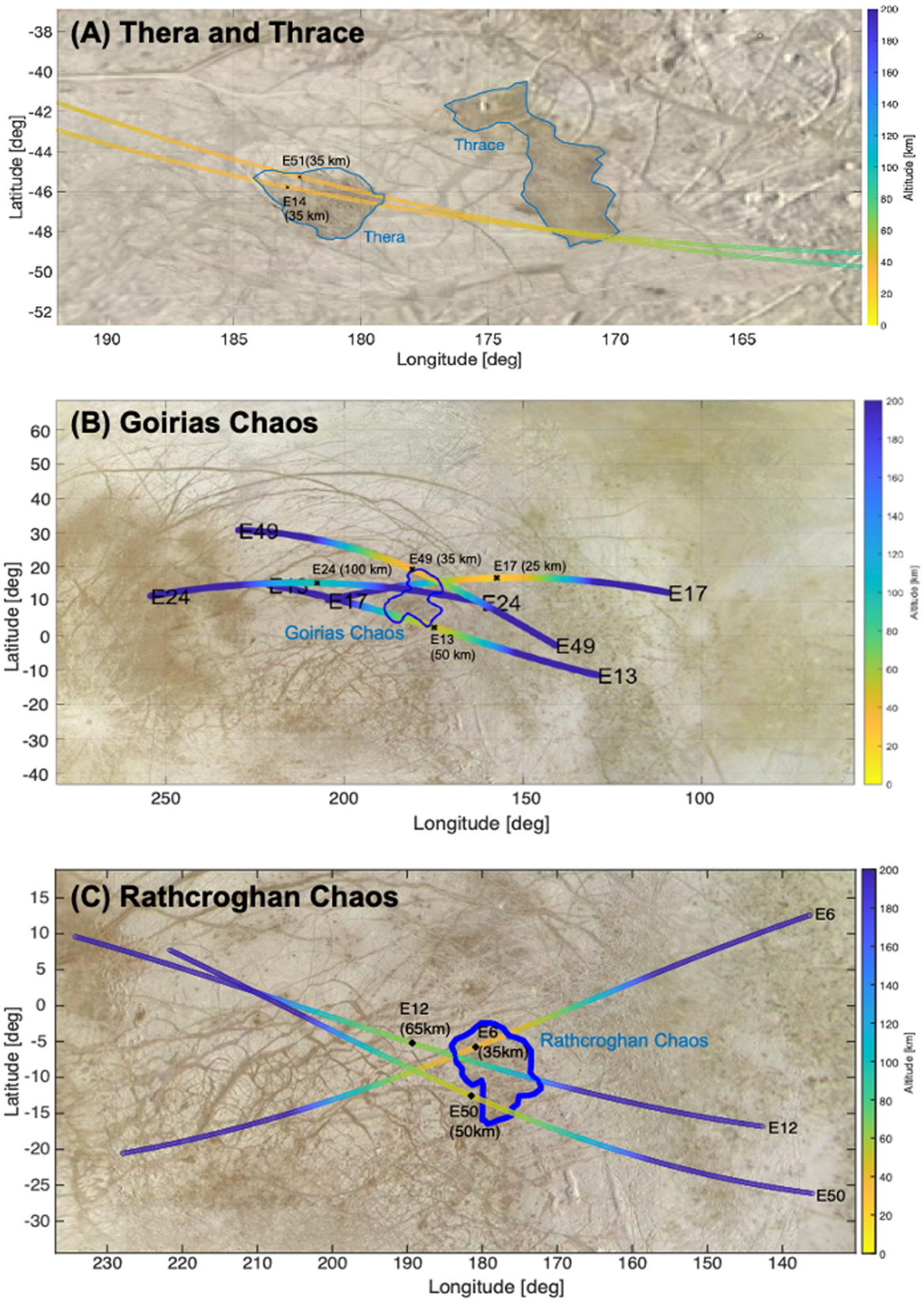

Figure 10. Crossover flybys over selected young geological terrains provide repeated coverage for SUDA to perform compositional mapping and monitor changes in between flybys. (a) E14 and E51 flybys provide the best coverage of Thera and partial coverage of Thrace; the later flyby would be in the extended mission. These two flybys are of top priority for the SUDA measurement plan. (b) Goirias Chaos will be studied during four flybys, providing an evenly timed coverage. (b) Rathcroghan Chaos will be studied during three flybys, with E6 providing the best coverage at 35 km altitude.

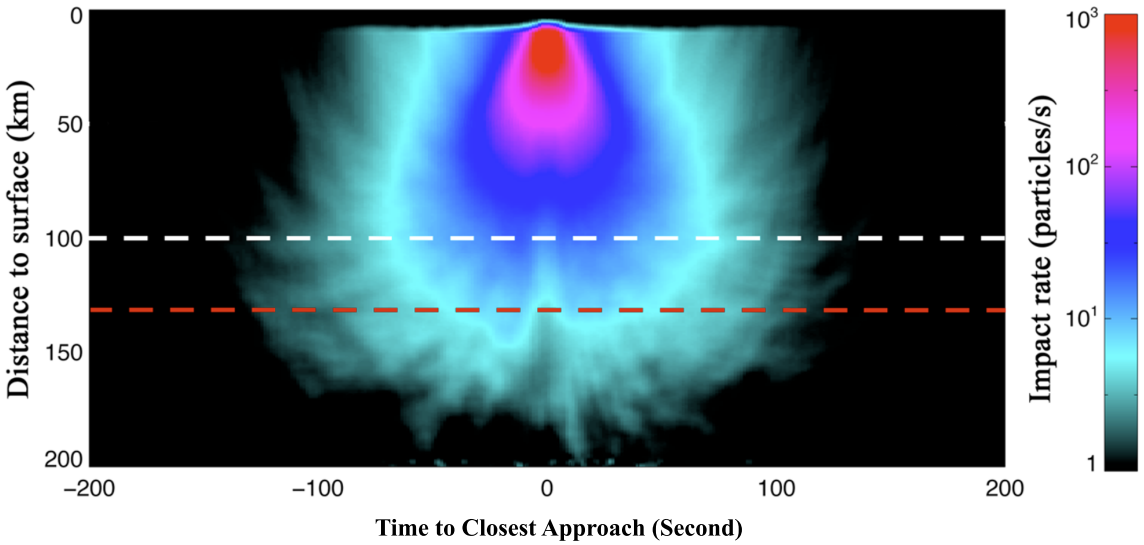

Figure 11. Simulated plume dust impact rate as a function of altitude above Europa. With a plume gas ejection speed of 700 m s^{-1}, plume grains are gravitationally bound and will fall back onto the surface in relatively close proximity to the source. For a reliable plume identification, an impact rate of ~10 s^{-1} is preferable, which translates to an altitude of 100–150 km above the plume source location. From B. S. Southworth et al. (2015).

4.9. REASON

The Radar for Europa Assessment and Sounding: Ocean to Near-surface (REASON) instrument is a dual-frequency—high frequency (HF) at 9 MHz and very high frequency (VHF) at 60 MHz center frequencies—ice-penetrating radar intended to study Europa from the exosphere to the subsurface ocean (O. Abramov & J. R. Spencer 2009; D. D. Blankenship et al. 2024). REASON transmits radar signals that propagate from the spacecraft toward Europa and reflect off contrasts in electromagnetic material properties (dielectric permittivity). The echoes are then recorded by REASON. As the radar signals traverse Europa's exosphere and interact with the moon's surface, they will be sensitive to localized anomalies associated with possible plumes.

Ionized ejecta from an active plume will increase the total electron content (TEC) in the vertical column between the spacecraft and Europa through which REASON signals propagate. This increased electron content will induce detectable dispersive phase shifts between the two REASON bands, as HF signals will be slowed relative to those in the VHF band (C. Grima et al. 2015). By characterizing the small changes in HF and VHF travel time from the spacecraft to the surface (K. M. Scanlan et al. 2019), REASON will be able to quantify the ionospheric TEC and the presence of local anomalies that can be related to plume activity. These altitude-integrated TEC measurements complement the local spacecraft ionospheric measurements from PIMS.

In parallel with detecting localized ionospheric anomalies due to plumes, surficial plume fallout deposits preserved on the surface of Europa can also be assessed by way of REASON reflectometry measurements. REASON reflectometry involves the characterization of Europa surface properties (e.g., dielectric permittivity, surface roughness, deposit thickness) from the strength of backscattered surface echoes. Initially developed to study the surface of Mars (C. Grima et al. 2012, 2022), reflectometry has also been applied to the study of Titan (C. Grima et al. 2017), as well as airborne and spaceborne radar measurements of Earth's ice sheets (C. Grima et al. 2014a, 2014b, 2016; A. Rutishauser et al. 2016; K. M. Scanlan et al. 2023). Assuming a near surface mostly composed of ice-rich materials, dielectric permittivity derived from radar reflectometry can then be linked to surface density and, equivalently, porosity. Local variations in these properties across Europa's surface can be used to indicate the presence of a plume deposit (i.e., reduced density, lower surface roughness). However, changes in deposit thickness can complicate this relationship (K. M. Scanlan et al. 2022). Surface properties (such as porosity) derived through REASON reflectometry along Europa Clipper ground tracks will complement the surface thermal properties extracted from E-THEMIS and MISE measurements.

4.10. G/RS

The Gravity/Radio Science investigation (G/RS) utilizes the telecommunications signal between Earth-based observing ground stations and the Europa Clipper spacecraft (E. Mazarico et al. 2023). Specifically for Europa's environment, the G/RS investigation measures vertical profiles of ionospheric electron density via radio occultation observation. Radio occultations are a common method for making remote-sensing measurements of vertical profiles of ionospheric electron density at solar system objects (e.g., P. Withers 2010; P. W. Withers et al. 2014, 2020; P. A. Dalba & P. Withers 2019). In such observations, a radio signal is sent from a transmitter to a receiver at a time when the ray path between transmitter and receiver passes through the ionosphere and atmosphere of a target object. The radio frequency received at the ground station is affected by refraction in the ionosphere of the target object, leading to a "frequency residual" between observed and predicted values.

At present, there are 10 ionospheric electron density profiles obtained through radio occultations by the Galileo spacecraft at Europa (A. J. Kliore et al. 1997). These profiles are generally consistent with the hypothesis that electron densities are depleted in the magnetospheric wake region and enhanced on the magnetospheric flanks, but they are not sufficient to test this hypothesis. Noted that a high electron density was inferred during a Galileo occultation that probed a region

where indications for plumes were derived from HST data (W. B. Sparks et al. 2017).

G/RS radio occultation observations will measure the spatial distribution and temporal evolution of Europa's ionospheric electron density. Similar to REASON, G/RS measurements can detect ionized ejecta from an active plume through locally increased electron content in the ionosphere. While REASON probes the vertical column density, G/RS obtains horizontal line-of-sight measurements of the electron content. G/RS measurements of localized enhancements in electron density could indicate a possible active plume.

5. Europa Clipper Plume Search Strategy

The Europa Clipper science team has adopted a global plume search strategy not focusing on any area or any type of observation, due to the lack of unequivocal evidence for the presence of a plume at Europa (Section 3). As such, in the current science and operations planning, plume search observations rely on diverse measurements and techniques (Table 1). For example, plans include spatially distributed imaging at different illumination conditions, observing stellar occultations from a variety of viewing geometries, and monitoring of in situ data for any opportunistic detections. This global and diverse data set strategy also means that collecting these data toward the beginning of the mission is important in that if plumes are discovered or confirmed there will be time for further investigation and characterization later in the mission.

Europa Clipper's various investigations contribute to plume search in different ways (Section 4), and the variety of resulting data sets helps to maximize the ability to detect any potential plume with currently unknown characteristics. Currently active plumes could be detected with the optical remote-sensing investigations EIS, MISE, E-THEMIS, and Europa-UVS via imaging or occultation, while E-THEMIS could detect its surface heat signature. REASON, along with the in situ investigations ECM and PIMS and the G/RS investigation, would detect perturbations in the magnetic field and plasma environment, and MASPEX and SUDA would detect enhancements or changes in the composition in the exosphere and dust population caused by an active plume. Recent or inactive plumes could be primarily detected through remote sensing of plume deposits with EIS, MISE, Europa-UVS, E-THEMIS, or REASON depending on the plume deposit characteristics. Ejecta from plume deposits could also be investigated by SUDA during close flybys, and MASPEX may detect remaining signatures in the atmosphere.

The characteristics of the potential Europan plumes cannot be known until a plume is confidently detected and characteristics observationally constrained. Given the absence of firm and direct plume detections in previous spacecraft data and difficulties in obtaining confirmed telescopic detections, confirmation of a potential plume would likely require several lines of evidence, including some or all of the following: (1) repeat direct observations, (2) direct detections with multiple investigations, (3) evidence that the anomaly was not associated with an impact event, (4) endogenic thermal emission or other activity at the plume source locations, and (5) surface change detection due to plume deposits. Confirming a plume detection would potentially result in a need for increased data downlink, reprioritization of downlink products, follow-up telescopic observations (e.g., by JWST), or other spacecraft observations (e.g., by the Jupiter Icy Moon Explorer of the European Space Agency; O. Grasset et al. 2013). Additionally, depending on the characteristics of the inferred plume, a potential detection could change the distant plume search strategy, or affect different instrument settings (e.g., MASPEX mass regions of interest; Europa-UVS spectral/spatial trades).

Europa Clipper's currently planned Tour Phase (Figure 5) is generally divided up into four parts: Transition to Europa Campaign 1 (TEC1), Europa Campaign 1 (EC1), Transition to Europa Campaign 2 (TEC2), and Europa Campaign 2 (EC2). EC1 and EC2 denote when the closest approach of the spacecraft is predominantly on the anti-Jovian hemisphere and sub-Jovian hemisphere, respectively (warmer colors of the ground tracks near 0° and 180° longitude; Figure 5). The TEC1 and TEC2 portions occur as the Europa Clipper orbit is pumped down post–Jupiter Orbit Insertion and then as the orbit is adjusted to move from the closest approaches above the anti-Jovian hemisphere to the sub-Jovian hemisphere, respectively. While the transition phases are generally at very high altitudes with respect to Europa that preclude high-resolution and in situ measurements, they are of particular interest to the remote plume search with Europa-UVS, EIS, E-THEMIS, and MISE because they have unique lighting geometries and because TEC1 is the earliest part of the mission to start searching for plumes. Early plume detection is of particular interest because it would allow for the refinement of the plume search and characterization for the rest of the mission, as discussed above.

Each Europa flyby is divided up into two principal parts, nadir and non-nadir. The nadir portion of the flyby takes place ±2–3 hr around closest approach, during which the spacecraft is oriented to have all the remote-sensing instruments' boresights pointing nadir, or toward Europa's subspacecraft point. The non-nadir portion of the flyby is any part outside of the ±2–3 hr around closest approach, where the spacecraft is distant from Europa and pointed primarily so that the High Gain Antenna is oriented at Earth to downlink data collected during the nadir portion of the flyby, but the spacecraft can also be pointed to collect distant science data of Europa or calibration data.

During the nadir phase, the primary plume detection method will be with ECM and/or PIMS sensing disturbances in the magnetic and plasma environment, SUDA and/or MASPEX directly sampling material that is not consistent with Europa's sputtered (or sublimated) exosphere and meteoroid bombardment alone, or remotely by observing plume deposits with EIS, MISE, E-THEMIS, or REASON. During the non-nadir phase, plume activity may be detected remotely, such as through high phase angle or limb images with EIS, through auroral emission detections or stellar occultations with Europa-UVS, or during radio occultations with GR/S.

If a plume is detected and confirmed, revision of the global search strategy might be warranted as elaborated above. However, the global plume search would likely never be totally abandoned, even if a plume is potentially detected by telescopic observations or Clipper itself. Especially because plume detection on Europa has been elusive to date, understanding the frequency, distribution, and potential variation in plume activity across Europa will warrant continuation of the global plume search, at least during the prime mission.

Characterization may become more of the focus in the extended mission. The case of Cassini's detection of the plume at Enceladus (Section 3.5) showed an example where adjustments in the (extended) mission greatly enhanced the science return on plume characterization.

6. Summary

Over the past decade, several studies have interpreted a variety of remote and in situ observations as potential evidence for large vapor plumes at different locations on Europa. However, this evidence is elusive, and visible imaging data taken during flybys of the Voyager, Galileo, and Juno spacecraft do not reveal any certain indications of ongoing gas or particle eruptions.

After arriving in the Jovian system, NASA's Europa Clipper spacecraft will systematically search for and constrain plume activity utilizing a variety of investigations and methods. Plume-generating processes could give rise to three primary signatures detectable by Europa Clipper during an integrated plume search: water vapor and other vented gases, including their plasma and field effects; particles made of ice and other materials, including surface deposits of particles and condensed gases; and surface thermal anomalies ("hot spots"). The strength and duration of these detectable signatures will depend on a variety of factors, including plume size and composition, as well as eruption mechanism and duration.

Infrequent plume activity on small scales or recent resurfacing via other geological processes (I. J. Daubar et al. 2024) may go undetected, given the capabilities of the instruments on Europa Clipper and the design of the multiple-flyby mission as described above. However, if no signs of current activity have been detected by Europa Clipper by the end of the mission, this will provide the most stringent constraints on the scale and frequency of any possible phenomena to date. Moreover, previous tentative detections in remote-sensing and archival spacecraft data may need to be checked against the constraints by the Europa Clipper measurements and interpretations possibly revisited. For example, frequent (17% duty cycle) large (>50 km height) eruptions as suggested by W. B. Sparks et al. (2017) are likely to be detected by Europa Clipper in some way.

Given the lack of reproducible plume detections at Europa to date, Europa Clipper has adopted a global plume search strategy that does not focus on any specific geographical area or type of observation. Instead, plume search observations in the current science and operations planning are focused on breadth. This global plume search strategy assigns enhanced value to data obtained early in the mission in that this will allow time for further observations and characterization of any observed plumes at later times. If a plume(s) is (are) detected and confirmed, the global strategy might be reconsidered, taking into consideration the characteristics and relevance of new detection(s).

Acknowledgments

Portions of this research was carried out at the Jet Propulsion Laboratory, California Institute of Technology, under a contract with the National Aeronautics and Space Administration (80NM0018D0004). This work was supported in part by NASA through the Europa Clipper Project. L.R. is supported by the Swedish National Space Agency through grant 2021-00153.

ORCID iDs

Lorenz Roth https://orcid.org/0000-0003-0554-4691
Erin Leonard https://orcid.org/0000-0002-5150-5426
Kelly Miller https://orcid.org/0000-0001-5657-137X
Matt Hedman https://orcid.org/0000-0002-8592-0812
Lynnae C. Quick https://orcid.org/0000-0003-0123-2797
Tracy M. Becker https://orcid.org/0000-0002-1559-5954
Shawn Brooks https://orcid.org/0000-0001-8622-0829
Corey Cochrane https://orcid.org/0000-0002-4935-1472
Ashley Gerard Davies https://orcid.org/0000-0003-1747-8142
Carolyn M. Ernst https://orcid.org/0000-0002-9434-7886
Cyril Grima https://orcid.org/0000-0001-7135-3055
Candice J. Hansen https://orcid.org/0000-0001-5863-299X
Carly Howett https://orcid.org/0000-0003-1869-4947
Sean Hsu https://orcid.org/0000-0002-5478-4168
Xianzhe Jia https://orcid.org/0000-0002-8685-1484
Adrienn Luspay-Kuti https://orcid.org/0000-0002-7744-246X
Margaret Kivelson https://orcid.org/0000-0003-4497-8759
Fabian Klenner https://orcid.org/0000-0002-5744-1718
Alfred McEwen https://orcid.org/0000-0001-8638-2553
William B. McKinnon https://orcid.org/0000-0002-4131-6568
Robert T. Pappalardo https://orcid.org/0000-0003-2571-4627
Frank Postberg https://orcid.org/0000-0002-5862-4276
Julie Rathbun https://orcid.org/0000-0001-7619-652X
Kurt D. Retherford https://orcid.org/0000-0001-9470-150X
Kirk Scanlan https://orcid.org/0000-0002-6483-0092
K. Marshall Seaton https://orcid.org/0000-0002-4202-7602
John R. Spencer https://orcid.org/0000-0003-4452-8109
J. Hunter Waite https://orcid.org/0000-0002-1978-1025
Paul Withers https://orcid.org/0000-0003-3084-4581
Danielle Wyrick https://orcid.org/0000-0003-3625-4267
Mikhail Yu. Zolotov https://orcid.org/0000-0003-0670-0684

References

Abramov, O., & Spencer, J. R. 2009, Endogenic Heat from Enceladus' South Polar Fractures: New Observations, and Models of Conductive Surface Heating, Icar, 199, 189
Arnold, H., Liuzzo, L., & Simon, S. 2019, Magnetic Signatures of a Plume at Europa during the Galileo E26 Flyby, GeoRL, 46, 1149
Becker, T. M., Zolotov, M. Y., Gudipati, M. S., et al. 2024, Exploring the Composition of Europa with the Upcoming Europa Clipper Mission, SSRv, 220, 49
Bennett, K. A., Hill, J. R., Murray, K. C., et al. 2018, THEMIS-VIS Investigations of Sand at Gale Crater, E&SS, 5, 352
Blaney, D., Hibbitts, K., Diniega, S., et al. 2024, The Mapping Imaging Spectrometer for Europa (MISE), SSRv, 220, 80
Blankenship, D. D., et al. 2024, Radar for Europa Assessment and Sounding: Ocean to Near-Surface (REASON), SSRv, 220
Blöcker, A., Saur, J., & Roth, L. 2016, Europa's Plasma Interaction with an Inhomogeneous Atmosphere: Development of Alfvén Winglets within the Alfvén Wings, JGRA, 121, 9794
Bouquet, A., Glein, C. R., & Waite, J. H. 2019, How Adsorption Affects the Gas–Ice Partitioning of Organics Erupted from Enceladus, ApJ, 873, 28
Brown, M. E., & Hand, K. P. 2013, Salts and Radiation Products on the Surface of Europa, AJ, 145, 110
Cable, M. L., Porco, C., Glein, C. R., et al. 2021, The Science Case for a Return to Enceladus, PSJ, 2, 132
Cassidy, T., Paranicas, C., Shirley, J., et al. 2013, Magnetospheric Ion Sputtering and Water Ice Grain Size at Europa, P&SS, 77, 64
Cassidy, T. A., Johnson, R. E., & Tucker, O. J. 2009, Trace Constituents of Europa's Atmosphere, Icar, 201, 182

Christensen, P. R., Spencer, J. R., Mehall, G. L., et al. 2024, The Europa Thermal Emission Imaging System (E-THEMIS) Investigation for the Europa Clipper Mission, SSRv, 220, 1
Collins, S. A. 1981, Spatial Color Variations in the Volcanic Plume at Loki, on Io, JGR, 86, 8621
Combe, J. P., McCord, T. B., Matson, D. L., et al. 2019, Nature, Distribution and Origin of CO_2 on Enceladus, Icar, 317, 491
Cook, A. F., Shoemaker, E. M., & Smith, B. A. 1979, Dynamics of Volcanic Plumes on Io, Natur, 280, 743
Cordiner, M. A., Thelen, A. E., Lai, I. L., et al. 2024, arXiv:2404.05525
Dalba, P. A., & Withers, P. 2019, Cassini Radio Occultation Observations of Titan's Ionosphere: The Complete Set of Electron Density Profiles, JGRA, 124, 643
Dalton, J. B., III, Shirley, J. H., & Kamp, L. W. 2012, Europa's Icy Bright Plains and Dark Linea: Exogenic and Endogenic Contributions to Composition and Surface Properties, JGRE, 117, 1–16
Dong, Y., Hill, T., Teolis, B., Magee, B., & Waite, J. 2011, The Water Vapor Plumes of Enceladus, JGRA, 116, A10204
Daubar, I. J., Hayes, A. G., Collins, G. C., et al. 2024, Planned Geological Investigations of the Europa Clipper Mission, SSRv, 220, 18
Dougherty, M. K., Khurana, K. K., Neubauer, F. M., et al. 2006, Identification of a Dynamic Atmosphere at Enceladus with the Cassini Magnetometer, Sci, 311, 1406
Fagents, S. A. 2003, Considerations for Effusive Cryovolcanism on Europa: The Post-Galileo Perspective, JGRE, 108, 1–18
Fagents, S. A., Greeley, R., Sullivan, R. J., et al. 2000, Cryomagmatic Mechanisms for the Formation of Rhadamanthys Linea, Triple Band Margins, and Other Low-Albedo Features on Europa, Icar, 144, 54
Geissler, P. E., & McMillan, M. T. 2008, Galileo Observations of Volcanic Plumes on Io, Icar, 197, 505
Giono, G., Roth, L., Ivchenko, N., et al. 2020, An Analysis of the Statistics and Systematics of Limb Anomaly Detections in HST/STIS Transit Images of Europa, AJ, 159, 155
Glein, C. R., Baross, J. A., & Waite, J. H. 2015, The pH of Enceladus' Ocean, GeCoA, 162, 202
Glein, C. R., & Waite, J. H. 2020, The Carbonate Geochemistry of Enceladus' Ocean, GeoRL, 47, e2019GL085885
Glein, C. R., Zolotov, M. Y., & Shock, E. L. 2008, The Oxidation State of Hydrothermal Systems on Early Enceladus, Icar, 197, 157
Goguen, J. D., Buratti, B. J., Brown, R. H., et al. 2013, The Temperature and Width of an Active Fissure on Enceladus Measured with Cassini VIMS During the 14 April 2012 South Pole Flyover, Icar, 226, 1128
Goode, W., Kempf, S., & Schmidt, J. 2021, Detecting the Surface Composition of Geological Features on Europa and Ganymede using a Surface Dust Analyzer, P&SS, 208, 105343
Goode, W., Kempf, S., & Schmidt, J. 2023, Mapping the Surface Composition of Europa with SUDA, P&SS, 227, 105633
Grasset, O., Dougherty, M. K., Coustenis, A., et al. 2013, JUpiter ICy Moons Explorer (JUICE): An ESA Mission to Orbit Ganymede and to Characterise the Jupiter System, P&SS, 78, 1
Grima, C., Blankenship, D. D., & Schroeder, D. M. 2015, Radar Signal Propagation through the Ionosphere of Europa, P&SS, 117, 421
Grima, C., Blankenship, D. D., Young, D. A., & Schroeder, D. M. 2014a, Surface Slope Control on Firn Density at Thwaites Glacier, West Antarctica: Results from Airborne Radar Sounding, GeoRL, 41, 6787
Grima, C., Greenbaum, J. S., Lopez Garcia, E. J., et al. 2016, Radar Detection of the Brine Extent at McMurdo Ice Shelf, Antarctica, and Its Control by Snow Accumulation, GeoRL, 43, 7011
Grima, C., Kofman, W., Henrique, A., Orosei, R., & Seu, R. 2012, Quantitative Analysis of Mars Surface Radar Reflectivity at 20MHz, Icar, 220, 84
Grima, C., Mastrogiuseppe, M., Hayes, A. G., et al. 2017, Surface Roughness of Titan's Hydrocarbon Seas, E&PSL, 474, 20
Grima, C., Putzig, N. E., Campbell, B. A., et al. 2022, Investigating the Martian Surface at Decametric Scale: Population, Distribution, and Dimension of Heterogeneity from Radar Statistics, PSJ, 3, 236
Grima, C., Schroeder, D. M., Blankenship, D. D., & Young, D. A. 2014b, Planetary Landing-Zone Reconnaissance Using Ice-Penetrating Radar Data: Concept Validation in Antarctica, P&SS, 103, 191
Grundy, W. M., Buratti, B. J., Cheng, A. F., et al. 2007, New Horizons Mapping of Europa and Ganymede, Sci, 318, 234
Grün, E., Fechtig, H., Hanner, M. S., et al. 1992, The Galileo Dust Detector, SSRv, 60, 317
Hansen, C. J., Esposito, L., Stewart, A. I., et al. 2006, Enceladus' Water Vapor Plume, Sci, 311, 1422
Hansen, C. J., Esposito, L. W., & Hendrix, A. R. 2019, Ultraviolet Observation of Enceladus' Plume in Transit across Saturn, Compared to Europa, Icar, 330, 256
Hansen, C. J., Ravine, M. A., Schenk, P. M., et al. 2024, Juno's JunoCam Images of Europa, PSJ, 5, 76
Hansen, C. J., Shemansky, D. E., Esposito, L. W., et al. 2011, The Composition and Structure of the Enceladus Plume, GeoRL, 38, L11202
Hartogh, P., Lellouch, E., Moreno, R., et al. 2011, Direct Detection of the Enceladus Water Torus with Herschel, A&A, 532, L2
Hayne, P. O., Bandfield, J. L., Siegler, M. A., et al. 2017, Global Regolith Thermophysical Properties of the Moon from the Diviner Lunar Radiometer Experiment, JGRE, 122, 2371
Head, J. W., Pappalardo, R. T., & Sullivan, R. 1999, Europa: Morphological Characteristics of Ridges and Triple Bands from Galileo Data (E4 and E6) and Assessment of a Linear Diapirism Model, JGRE, 104, 24223
Hedman, M. M., Gosmeyer, C. M., Nicholson, P. D., et al. 2013, An Observed Correlation between Plume Activity and Tidal Stresses on Enceladus, Natur, 500, 182
Howett, C., Spencer, J., Pearl, J., & Segura, M. 2011, High Heat Flow from Enceladus' South Polar Region Measured Using 10–600 cm^{-1} Cassini/CIRS Data, JGRE, 126, E03003
Howett, C. J. A., Spencer, J. R., Hurford, T., Verbiscer, A., & Segura, M. 2012, PacMan Returns: An Electron-Generated Thermal Anomaly on Tethys, Icar, 221, 1084
Howett, C. J. A., Spencer, J. R., Hurford, T., Verbsicer, A., & Segura, M. 2014, Thermophysical Property Variation across Dione and Rhea, Icar, 241, 239
Howett, C. J. A., Spencer, J. R., Schenk, P., et al. 2011, A High-amplitude Thermal Anomaly of Probable Magnetospheric Origin on Saturn's Moon Mimas, Icar, 216, 221
Huybrighs, H. L. F., Roussos, E., Blöcker, A., et al. 2020, An Active Plume Eruption on Europa during Galileo Flyby E26 as Indicated by Energetic Proton Depletions, GeoRL, 47, e2020GL087806
Jia, X., Kivelson, M. G., Khurana, K. K., & Kurth, W. S. 2018, Evidence of a Plume on Europa from Galileo Magnetic and Plasma Wave Signatures, NatAs, 2, 459
Jia, X., Kivelson, M. G., & Paranicas, C. 2021, Comment on 'An Active Plume Eruption on Europa during Galileo Flyby E26 as Indicated by Energetic Proton Depletions' by Huybrighs et al, GeoRL, 48, e2020GL091550
Johnson, R. E., Burger, M. H., Cassidy, T. A., et al. 2009, Composition and Detection of Europa's Sputter-Induced Atmosphere, Europa, 21, 507
Kempf, S., Beckmann, U., & Schmidt, J. 2010, How the Enceladus Dust Plume Feeds Saturn's E Ring, Icar, 206, 446
Kempf, S., Tucker, S., Altobelli, N., et al. 2024, SUDA: A SUrface Dust Analyser for Compositional Mapping of the Galilean Moon Europa, SSRv, 221, 10
Khawaja, N., Postberg, F., Hillier, J., et al. 2019, Low-Mass Nitrogen-, Oxygen-bearing, and Aromatic Compounds in Enceladean Ice Grains, MNRAS, 489, 5231
Kieffer, S. W., Lu, X., Bethke, C. M., et al. 2006, A Clathrate Reservoir Hypothesis for Enceladus' South Polar Plume, Sci, 314, 1764
Kimura, J., Matsuo, T., Kobayashi, H., et al. 2024, A Search for Water Vapor Plumes on Europa by Spatially Resolved Spectroscopic Observation Using Subaru/IRCS, PASJ, 76, 1302
Kivelson, M. G., Jia, X., Lee, K., et al. 2023, The Europa Clipper Magnetometer, SSRv, 219, 48
Klenner, F., Bönigk, J., Napoleoni, M., et al. 2024, How to Identify Cell Material in a Single Ice Grain Emitted from Enceladus or Europa, SciA, 10, eadl0849
Klenner, F., Postberg, F., Hillier, J., et al. 2020, Discriminating Abiotic and Biotic Fingerprints of Amino Acids and Fatty Acids in Ice Grains Relevant to Ocean Worlds, AsBio, 20, 1168
Kliore, A. J., Hinson, D. P., Flasar, F. M., Nagy, A. F., & Cravens, T. E. 1997, The Ionosphere of Europa from Galileo Radio Occultations, Sci, 277, 355
Krivov, A. V., Sremčević, M., Spahn, F., Dikarev, V. V., & Kholshevnikov, K. V. 2003, Impact-Generated Dust Clouds around Planetary Satellites: Spherically Symmetric Case, P&SS, 51, 251
Krüger, H., Grün, E., Heck, A., & Lammers, S. 1999, Analysis of the Sensor Characteristics of the Galileo Dust Detector with Collimated Jovian Dust Stream Particles, P&SS, 47, 1015
Krüger, H., Krivov, A. V., & Grün, E. 2000, A Dust Cloud of Ganymede Maintained by Hypervelocity Impacts of Interplanetary Micrometeoroids, P&SS, 48, 1457
Krüger, H., Krivov, A. V., Sremčević, M., & Grün, E. 2003, Impact-Generated Dust Clouds Surrounding the Galilean Moons, Icar, 164, 170

Lagg, A., Krupp, N., Woch, J., & Williams, D. J. 2003, In-Situ Observations of a Neutral Gas Torus at Europa, GeoRL, 30, 11
Leonard, E. J., Patthoff, D. A., & Senske, D. A. 2024, Global Geologic Map of Europa, Vol. 3513 (Reston, VA: US Geological Survey)
Lesage, E., Massol, H., Howell, S. M., & Schmidt, F. 2022, Simulation of Freezing Cryomagma Reservoirs in Viscoelastic Ice Shells, PSJ, 3, 170
Matteoni, P., Neesemann, A., Jaumann, R., Hillier, J., & Postberg, F. 2023a, Evolution of Thrace Macula on Europa: Strike-Slip Tectonic Control and Identification of the Youngest Terrains, JGRE, 128, e2023JE007905
Matteoni, P., et al. 2023b, Ménec Fossae on Europa: A Strike-Slip Tectonics Origin above a Possible Shallow Water Reservoir, JGRE, 128, e2022JE007623
Mauk, B. H., Mitchell, D. G., Krimigis, S. M., Roelof, E. C., & Paranicas, C. P. 2003, Energetic Neutral Atoms from a Trans-Europa Gas Torus at Jupiter, Natur, 421, 920
Mazarico, E., Buccino, D., Castillo-Rogez, J., et al. 2023, The Europa Clipper Gravity and Radio Science Investigation, SSRv, 219, 30
Nelson, R. M., Smythe, W. D., Hapke, B. W., & Hale, A. S. 2002, Low Phase Angle Laboratory Studies of the Opposition Effect: Search for Wavelength Dependence, P&SS, 50, 849
Nénon, Q., & Leblanc, F. 2024, The Neutral Water Torus of Europa, GeoRL, 51, e2024GL112110
Paganini, L., Villanueva, G. L., Roth, L., et al. 2020, A Measurement of Water Vapour amid a Largely Quiescent Environment on Europa, NatAs, 4, 266
Pappalardo, R. T., Belton, M. J., Breneman, H. H., et al. 1999, Does Europa Have a Subsurface Ocean? Evaluation of the Geological Evidence, JGRE, 104, 24015
Pappalardo, R. T., Buratti, B. J., Korth, H., et al. 2024, Science Overview of the Europa Clipper Mission, SSRv, 220, 40
Perry, M. E., Teolis, B. D., Hurley, D. M., et al. 2015, Cassini INMS Measurements of Enceladus Plume Density, Icar, 257, 139
Phillips, C. B., McEwen, A. S., Hoppa, G. V., et al. 2000, The Search for Current Geologic Activity on Europa, JGRE, 105, 22579
Porco, C. C., Helfenstein, P., Thomas, P. C., et al. 2006, Cassini Observes the Active South Pole of Enceladus, Sci, 311, 1393
Postberg, F., Clark, R. N., Hansen, C. J., et al. 2018a, Plume and Surface Composition of Enceladus, in Enceladus and the Icy Moons of Saturn, ed. P. M. Schenk et al. (Tucson, AZ: Univ. Arizona Press), 129
Postberg, F., Khawaja, N., Abel, B., et al. 2018b, Macromolecular Organic Compounds from the Depths of Enceladus, Natur, 558, 564
Postberg, F., Schmidt, J., Hillier, J., Kempf, S., & Srama, R. 2011, A Salt-Water Reservoir as the Source of a Compositionally Stratified Plume on Enceladus, Natur, 474, 620
Prockter, L. M., & Patterson, G. W. 2009, Morphology and Evolution of Europa's Ridges and Bands, Europa (Tucson, AZ: Univ. Arizona Press), 237
Quick, L. C., Barnouin, O. S., Prockter, L. M., & Patterson, G. W. 2013, Constraints on the Detection of Cryovolcanic Plumes on Europa, P&SS, 86, 1
Quick, L. C., & Hedman, M. M. 2020, Characterizing Deposits Emplaced by Cryovolcanic Plumes on Europa, Icar, 343, 113667
Rathbun, J., Spencer, J., Tamppari, L., et al. 2004, Mapping of Io's Thermal Radiation by the Galileo Photopolarimeter–Radiometer (PPR) Instrument, Icar, 169, 127
Rathbun, J. A., & Spencer, J. R. 2020, Proposed Plume Source Regions on Europa: No Evidence for Endogenic Thermal Emission, Icar, 338, 113500
Ravine, M. A., Hansen, C. J., Caplinger, M. A., et al. 2025, JunoCam Observations of Io, JGR, in press
Retherford, K. D., Becker, T. M., Gladstone, G. R., et al. 2024, Europa Ultraviolet Spectrograph (Europa-UVS), SSRv, 220, 89
Rhoden, A. R., Hurford, T. A., Roth, L., & Retherford, K. 2015, Linking Europa's Plume Activity to Tides, Tectonics, and Liquid Water, Icar, 253, 169
Roth, L., Ivchenko, N., Becker, T., et al. 2022, Europa's UV Emissions from 2014–2020: Molecular Atmosphere, Hydrogen Corona and Constraints on Plumes, in Magnetosphere of Outer Planets Meeting, Liege, Belgium, July 2022
Roth, L., Retherford, K. D., Saur, J., et al. 2014a, Orbital Apocenter Is Not a Sufficient Condition for HST/STIS Detection of Europa's Water Vapor Aurora, PNAS, 111, E5123
Roth, L., Saur, J., Retherford, K. D., Strobel, D. F., & Spencer, J. R. 2011, Simulation of Io's Auroral Emission: Constraints on the Atmosphere In Eclipse, Icar, 214, 495
Roth, L., Saur, J., Retherford, K. D., et al. 2014b, Transient Water Vapor at Europa's South Pole, Sci, 343, 171
Roth, L., Smith, H. T., Yoshioka, K., et al. 2023, Constraints on Europa's Water Group Torus from HST/COS Observations, PSJ, 4, 87
Rutishauser, A., Grima, C., Sharp, M., et al. 2016, Characterizing Near-surface Firn Using the Scattered Signal Component of the Glacier Surface Return from Airborne Radio-Echo Sounding, GeoRL, 43, 12502
Scanlan, K. M., Grima, C., Steinbrügge, G., et al. 2019, Geometric Determination of Ionospheric Total Electron Content from Dual Frequency Radar Sounding Measurements, P&SS, 178, 104696
Scanlan, K. M., Rutishauser, A., & Simonsen, S. B. 2023, Observing the Near-surface Properties of the Greenland Ice Sheet, GeoRL, 50, e2022GL101702
Scanlan, K. M., Young, D. A., & Blankenship, D. D. 2022, Non-Linear Radar Response to the Radial Structure of Europa Plume Fallout Deposits, Icar, 378, 114935
Schenk, P. M. 2020, The Search for Europa's Plumes: No Surface Patterns or Changes 1979–2007?, ApJL, 892, L12
Schmidt, J., Brilliantov, N., Spahn, F., & Kempf, S. 2008, Slow Dust in Enceladus' Plume from Condensation and Wall Collisions in Tiger Stripe Fractures, Natur, 451, 685
Smith, B. A., Soderblom, L. A., Johnson, T. V., et al. 1979, The Jupiter System through the Eyes of Voyager 1, Sci, 204, 951
Smith, H., Johnson, R., Perry, M., et al. 2010, Enceladus Plume Variability and the Neutral Gas Densities in Saturn's Magnetosphere, JGRA, 115
Smith, H. T., Mitchell, D. G., Johnson, R. E., Mauk, B. H., & Smith, J. E. 2019, Europa Neutral Torus Confirmation and Characterization Based on Observations and Modeling, ApJ, 871, 69
Southworth, B. S., Kempf, S., & Schmidt, J. 2015, Modeling Europa's Dust Plumes, GeoRL, 42, 10
Sparks, W. B., Hand, K. P., McGrath, M. A., et al. 2016, Probing for Evidence of Plumes on Europa with HST/STIS, ApJ, 826, 121
Sparks, W. B., Richter, M., deWitt, C., et al. 2019, A Search for Water Vapor Plumes on Europa Using SOFIA, ApJL, 871, L5
Sparks, W. B., Schmidt, B. E., McGrath, M. A., et al. 2017, Active Cryovolcanism on Europa?, ApJL, 839, L18
Spencer, J., Nimmo, F., Ingersoll, A. P., et al. 2018, Plume Origins and Plumbing: From Ocean to Surface, Enceladus and the Icy Moons of Saturn (Tucson, AZ: Univ. Arizona Press), 163
Spencer, J., Pearl, J., Segura, M., et al. 2006, Cassini Encounters Enceladus: Background and the Discovery of a South Polar Hot Spot, Sci, 311, 1401
Spencer, J. R., Barr, A. C., Esposito, L. W., et al. 2009, Enceladus: An Active Cryovolcanic Satellite, in Saturn from Cassini-Huygens, ed. M. K. Dougherty, L. W. Esposito, & S. M. Krimigis (Dordrecht: Springer), 683
Spencer, J. R., Stern, S. A., Cheng, A. F., et al. 2007, Io Volcanism Seen by New Horizons: A Major Eruption of the Tvashtar Volcano, Sci, 318, 240
Spitale, J. N., & Porco, C. C. 2007, Association of the Jets of Enceladus with the Warmest Regions on Its South-polar Fractures, Natur, 449, 695
Sremčević, M., Krivov, A. V., Krüger, H., & Spahn, F. 2005, Impact-Generated Dust Clouds around Planetary Satellites: Model versus Galileo Data, P&SS, 53, 625
Sremčević, M., Krivov, A. V., & Spahn, F. 2003, Impact-Generated Dust Clouds around Planetary Satellites: Asymmetry Effects, P&SS, 51, 455
Steinbrügge, G., Voigt, J. R., Wolfenbarger, N. S., et al. 2020a, Brine Migration and Impact-Induced Cryovolcanism on Europa, GeoRL, 47, e2020GL090797
Steinbrügge, G., Voigt, J. R. C., Schroeder, D. M., et al. 2020b, The Surface Roughness of Europa Derived from Galileo Stereo Images, Icar, 343, 113669
Teolis, B., Perry, M., Magee, B., Westlake, J., & Waite, J. 2010, Detection and Measurement of Ice Grains and Gas Distribution in the Enceladus Plume by Cassini's Ion Neutral Mass Spectrometer, JGRA, 115
Teolis, B. D., Perry, M. E., Hansen, C. J., et al. 2017a, Enceladus Plume Structure and Time Variability: Comparison of Cassini Observations, AsBio, 17, 926
Teolis, B. D., Wyrick, D. Y., Bouquet, A., Magee, B. A., & Waite, J. H. 2017b, Plume and Surface Feature Structure and Compositional Effects on Europa's Global Exosphere: Preliminary Europa Mission Predictions, Icar, 284, 18
Trumbo, S. K., & Brown, M. E. 2023, The Distribution of CO_2 on Europa Indicates an Internal Source of Carbon, Sci, 381, 1308
Trumbo, S. K., Brown, M. E., & Butler, B. J. 2018, ALMA Thermal Observations of Europa, AJ, 156, 161
Trumbo, S. K., Brown, M. E., & Hand, K. P. 2019, H_2O_2 Within Chaos Terrain on Europa's Leading Hemisphere, AJ, 158, 127
Turtle, E. P., McEwen, A. S., Patterson, G. W., et al. 2024, The Europa Imaging System (EIS) Investigation, SSRv, 220, 91

Vance, S. D., Craft, K. L., Shock, E., et al. 2023, Investigating Europa's Habitability with the Europa Clipper, SSRv, 219, 81
Velez, M. A., Retherford, K. D., Hue, V., et al. 2024, Catalog of Ultraviolet Bright Stars (CUBS): Strategies for UV Occultation Measurements, Planetary Illumination Modeling, and Sky Map Analyses Using Hybrid IUE–Kurucz Spectra, PSJ, 5, 93
Villanueva, G. L., Hammel, H. B., Milam, S. N., et al. 2023, Endogenous CO_2 Ice Mixture on the Surface of Europa and no Detection of Plume Activity, Sci, 381, 1305
Volwerk, M., Kivelson, M. G., & Khurana, K. K. 2001, Wave Activity in Europa's Wake: Implications for Ion Pick-Up, JGR, 106, 26033
Vorburger, A., & Wurz, P. 2021, Modeling of Possible Plume Mechanisms on Europa, JGRA, 126, e2021JA029690
Waite, J. H., Jr., Burch, J. L., Brockwell, T. G., et al. 2024, MASPEX-Europa: The Europa Clipper Neutral Gas Mass Spectrometer Investigation, SSRv, 220, 30
Waite, J. H., Combi, M. R., Ip, W.-H., et al. 2006, Cassini Ion and Neutral Mass Spectrometer: Enceladus Plume Composition and Structure, Sci, 311, 1419
Waite, J. H., Glein, C. R., Perryman, R. S., et al. 2017, Cassini Finds Molecular Hydrogen in the Enceladus Plume: Evidence for Hydrothermal Processes, Sci, 356, 155
Waite, J. H., Jr., Lewis, W., Magee, B., et al. 2009, Liquid Water on Enceladus from Observations of Ammonia and 40Ar in the Plume, Natur, 460, 487
Walker, C. C., & Schmidt, B. E. 2018, Investigating Active Chaos Formation as the Source of Europa's Water Vapor Plumes, LPSC, 49, 1302
Westlake, J., McNutt, R. L., Jr., Grey, M., et al. 2023, The Plasma Instrument for Magnetic Sounding (PIMS) on the Europa Clipper Mission, SSRv, 219, 62
Withers, P. 2010, Prediction of Uncertainties in Atmospheric Properties Measured by Radio Occultation Experiments, AdSpR, 46, 58
Withers, P. W., Felici, M., Mendillo, M., et al. 2020, The MAVEN Radio Occultation Science Experiment (ROSE), SSRv, 216, 61
Withers, P. W., Moore, L., Cahoy, K., & Beerer, I. 2014, How to Process Radio Occultation Data: 1. From Time Series of Frequency Residuals to Vertical Profiles of Atmospheric and Ionospheric Properties, P&SS, 101, 77
Yeoh, S. K., Li, Z., Goldstein, D. B., et al. 2017, Constraining the Enceladus Plume Using Numerical Simulation and Cassini Data, Icar, 281, 357